Comparing Step Potential Free Energy Approximations made with Fundamental Measure Theory

Bachelorarbeit aus der Physik

Vorgelegt von
Mishael Derla
11.04.2023

Institut für Theoretische Physik I
Friedrich-Alexander-Universität Erlangen-Nürnberg

Betreuer: Prof. Dr. Michael Schmiedeberg

Abstract

Ways of approximating the Helmholtz free energy functional (in the context of Classical Density Functional Theory) of the step potential $u_\mathrm{s}(r) = h\,\Theta(L-r)$ are derived, which are formulated with Fundamental Measure Theory. The first approach adds an interaction energy term to the White Bear II hard sphere gas excess free energy, where the weighted densities inserted into White Bear II are reweighted in a manner motivated by the Barker-Henderson effective hard sphere diameter. The second approach emulates Rosenfelds derivation of his original Fundamental Measure Theory, followed by a modification analogous to the changes White Bear II makes relative to Rosenfelds original functional.

Both analytically reproduce White Bear II for $\beta h \to \infty$ and the ideal gas for $\beta h \to 0$. Their behaviour is probed by comparing their predicted structure function with Monte Carlo simulations and with the Percus-Yercick closure to the Ornstein-Zernike equation. The Barker-Henderson + energy approach predicts a structure function in close agreement with the Percus-Yervick closure. The emulation of Rosenfeld's approach turns out to be sensitive to the quality of the approximation of interaction energy and in the approximations considered fails at intermediate step sizes $1 \lesssim \beta h \lesssim 3$. There are indications in its qualitative behaviour however, that suggest it includes effects seen in Monte Carlo simulations, that neither Percus-Yervick closure nor the first approach encompass.

Acknowledgments

I want to sincerely thank Prof. Michael Schmiedeberg for the supervision I received during this bachelor's thesis. He was very approachable and helpful anytime I required help with both conceptual and technical difficulties.

I also want to thank Matthias Gimperlein and Robert Weigel for many a helpful discussion on the theory involved. Further I want to thank Robert Weigel for the provision of Monte-Carlo computed structure functions and Matthias Gimperlein for the provision of direct correlation functions and structure functions computed via Ornstein-Zernike closures. Both datasets were essential guidance and the basis for my assessment of the results.

Contents

1 Motivation

The hard sphere gas is a very important reference system in the theory of fluids. The simplicity of the model allows useful approximations and via these closed expressions for many thermodynamic quantities. A framework for producing these is Fundamental Measure Theory.

The crudest soft interaction ("soft" as in not the hard sphere gas) describing non-vanishing $-\partial u/\partial r$ is the step potential

$$u_{\mathrm{s}}(r) := h\,\Theta(L-r)$$

where L is the distance at which the particles interact and h is the energy cost of closing in to distances below L; for its weak derivative, which can be interpreted as interparticle force, is $-\partial u_{\mathrm{s}}/\partial r = h\,\delta(L-r)$, a force acting at exactly one distance.

Since $\Theta(L-r)^k = \Theta(L-r)$ for any number k, given Θ takes on only the values 0 and 1, and since $e^x - 1 = x + \frac{1}{2}x^2 + \frac{1}{6}x^3 + \cdots$ contains only powers of x, the Mayer-f function of the step potential looks very similar to that of a hard sphere gas with sphere diameter L, $f_{\mathrm{h}}(r) = -\Theta(L-r)$, is in fact proportional to it

$$f_{\mathrm{s}}(r) = e^{-\beta u_{\mathrm{s}}} - 1 = \left(e^{-\beta h} - 1\right)\,\Theta(L-r)$$

Fundamental Measure Theory, as will be explained, relies on a decomposition of $\Theta(L-r)$ into cross correlations of geometrically well interpretable weights. Thus an attempt to apply its techniques to this apparently similar problem is motivated.

2 Theoretical Background

2.1 Classical Density Functional Theory

Classical Density Functional Theory is a way to tackle situations in statistical physics, in which the particle number density of a system is not homogeneous and said inhomogeneity is of physical interest. It is based on a result by Mermin [6], which states that no matter what the external potential $v(\boldsymbol{r})$ might be, there exists a functional $J[n]$ of *local particle number density*

$$n(\boldsymbol{r}) := N \cdot \langle \delta(\boldsymbol{x} - \boldsymbol{r}) \rangle \tag{1}$$

independent of $v(\boldsymbol{r})$, such that the functional

$$\Omega[n] = \int \mathrm{d}^3 r \, v(\boldsymbol{r}) \, n(\boldsymbol{r}) + J[n] \tag{2}$$

is minimized by the density profile $n_{\mathrm{eq}}(\boldsymbol{r})$ of equilibrium, at which point $\Omega[n]$ takes on the value of that equilibrium's grand potential[1].

Being $v(\boldsymbol{r})$-independent, J encodes ideal-gas- and interparticle interaction contributions to the grand potential. The existence of J translates into the existence of a density profile functional for the system's (Helmholtz) Free Energy F by its definition

$$F = \Omega + \mu N \tag{3}$$

Explicitly, F is promoted to a functional by

$$F[n] = \Omega[n] + \mu \int \mathrm{d}^3 r \; n(\boldsymbol{r}) \tag{4}$$

Its exact computation is unfeasible for all but the simplest cases, thus the study of its approximations. For the ideal gas[2] it turns out [4], that

$$\beta F_{\mathrm{id}}[n] = \int \mathrm{d}^3 r \; \big(n(\boldsymbol{r}) \log\big(\Lambda^3 n(\boldsymbol{r})\big) - n(\boldsymbol{r}) \big) \tag{5}$$

---

[1] Given a fixed $F[n]$, the possible n_{eq} are in one to one correspondence with the external potentials [6]

[2] The (grand canonical) ideal gas partition function is $Z_{\mathrm{id}} = \exp\big(z \cdot V/\Lambda^3\big)$, where $z = e^{\beta\mu}$. Now $n = \beta p = -\beta\Omega_{\mathrm{id}}/V = z \cdot 1/\Lambda^3$ and $\mu = \partial F_{\mathrm{id}}/\partial N$. By rearranging, one thus gets $\beta \, \partial F_{\mathrm{id}}/\partial N = \beta\mu = \log\big(\Lambda^3 n\big)$. Convincing oneself, that $\lim_{n\to 0} F_{\mathrm{id}} = 0$ finally results in $\beta F_{\mathrm{id}}/V = \big(n \log(\Lambda^3 n) - n\big)$

where $\Lambda = h/\sqrt{2\pi mkT}$ is the so called thermal de Broglie wavelength [8], which is related to the ideal gas by its partition function $Z_{\text{id}}(\beta, V, \mu) = \exp\left(e^{\beta\mu} \cdot V/\Lambda^3\right)$.

Now, given a classical system not in an external potential with a spherically symmetric pair interaction, the ideal gas is thought of as a reference system relative to which the interacting system has an *excess free energy* F_{ex}, i.e.

$$F[n] =: F_{\text{id}}[n] + F_{\text{ex}}[n] \tag{6}$$

The usefulness of that split goes beyond conceptual clarity, as is demonstrated by taking the variational derivative of (4) using (6), the minimality (and thus extremality) of $\Omega[n_{\text{eq}}]$ and the explicit expression for the ideal gas

$$\log(\Lambda^3 n_{\text{eq}}(\boldsymbol{r})) + \beta \frac{\delta F_{\text{ex}}}{\delta n(\boldsymbol{r})}[n_{\text{eq}}] = \beta\mu$$

$$\implies \Lambda^3 n_{\text{eq}}(\boldsymbol{r}) = \exp(\beta\mu) \exp\left(-\beta \frac{\delta F_{\text{ex}}}{\delta n(\boldsymbol{r})}[n_{\text{eq}}]\right) \tag{7}$$

meaning that knowledge of the excess free energy translates into an implicit expression for the particle number density profile $n_{\text{eq}}(\boldsymbol{r})$ in equilibrium and thus into knowledge of n_{eq}. In the case of the ideal gas, for example, where the excess free energy vanishes, (7) shows, that the equilibrium density profile is proportional to the imposed fugacity.

2.2 Fundamental Measure Theory

2.2.1 The Cross Correlation and Weighted Densities

Fundamental Measure Theory was kickstarted by Rosenfeld [10] in the study of the hard sphere gas (even mixtures of hard sphere gases of various radii, but mixtures will not be considered here). The foundational insight of its application to the hard sphere gas, is that the Mayer-f function $f(r) = -\Theta(2R - r)$, with hard sphere radius R, has the decomposition [4]

$$-f = \omega_0 \otimes \omega_3 + \omega_3 \otimes \omega_0 + \omega_1 \otimes \omega_2 + \omega_2 \otimes \omega_1 - \boldsymbol{\omega}_1 \otimes \boldsymbol{\omega}_2 - \boldsymbol{\omega}_2 \otimes \boldsymbol{\omega}_1 \tag{8}$$

The ω_α are called *weight functions* (for reasons obvious in a moment) and have the definitions

$$\omega_0(\boldsymbol{r}) := \frac{1}{R} \cdot \omega_1(\boldsymbol{r}) := \frac{1}{4\pi R^2} \cdot \omega_2(\boldsymbol{r}) := \frac{\delta(R - r)}{4\pi R^2} \tag{9}$$

$$\boldsymbol{\omega}_\alpha(\boldsymbol{r}) := \left(\frac{\boldsymbol{r}}{r}\right)\omega_\alpha \tag{10}$$

$$\omega_3(r) := \Theta(R - r) \tag{11}$$

$f \otimes g$ denotes not the tensor product but the cross correlation, an operation closely related to the convolution[3] which measures how alike two profiles f and g are when shifted by $\boldsymbol{q}$ to each other. It can be defined by [4]

$$f \otimes g(\boldsymbol{r}) := \int \mathrm{d}^3 q\, f(\boldsymbol{q})\, g(\boldsymbol{q} + \boldsymbol{r}) \tag{12}$$

where the product between the functions in the integrand is to be interpreted as the dot product in the case of vectorial functions. It has the property

$$f \otimes g(\boldsymbol{r}) = g \otimes f\,(-\boldsymbol{r}) \tag{13}$$

and transforms into Fourier space as[4]

$$\widehat{f \otimes g}(\boldsymbol{k}) = \hat{f}(-\boldsymbol{k}) \cdot \hat{g}(\boldsymbol{k}) \tag{14}$$

as is quickly deduced from (13) and the definition of the Fourier Transform.

Another insight is necessary, before elaboration on the ω_α's role can be made. In analogy to the expression for the second virial coefficient of spherically symmetric interaction potentials, the excess free energy functional expanded to second order in $n(\boldsymbol{r})$ (henceforth called the *the low density limit*) reads [10]

$$\beta F_{\mathrm{ex}}[n] \overset{n \to 0}{\approx} -\frac{1}{2} \int \mathrm{d}^3 r\, \mathrm{d}^3 q\; n(\boldsymbol{r})\, f(|\boldsymbol{r} - \boldsymbol{q}|)\, n(\boldsymbol{q}) \tag{15}$$

Inserting the hard sphere Mayer-f decomposition (8) into (15) along with using a coordinate shift to see, that

$$\omega_\alpha \otimes \omega_\beta(\boldsymbol{r}_i - \boldsymbol{r}_j) = \int \mathrm{d}^3 r\, \omega_\alpha(\boldsymbol{r} - \boldsymbol{r}_i)\, \omega_\beta(\boldsymbol{r} - \boldsymbol{r}_j) \tag{16}$$

and properly switching the order of integration, results in

$$-\frac{1}{2} \int\!\!\int \mathrm{d}^3 r\, \mathrm{d}^3 q\; n(\boldsymbol{r})\, f(|\boldsymbol{r} - \boldsymbol{q}|)\, n(\boldsymbol{q}) = \int \mathrm{d}^3 r (n_0 n_3 + n_1 n_2 - \boldsymbol{n}_1 \boldsymbol{n}_2) \tag{17}$$

---

[3] $g \mapsto f \otimes g$ is the transpose operator to $g \mapsto f * g$

[4] To see this, insert the Fourier decompositions of f and g into $f \otimes g(\boldsymbol{r})$ to get $\int \mathrm{d}^3 q \int\int \frac{\mathrm{d}^3 k_1}{(2\pi)^3} \frac{\mathrm{d}^3 k_2}{(2\pi)^3}\, e^{i\boldsymbol{k}_1 \boldsymbol{q}} e^{i\boldsymbol{k}_2(\boldsymbol{q}+\boldsymbol{r})} \hat{f}(\boldsymbol{k}_1) \hat{g}(\boldsymbol{k}_2)$ and use $\int \mathrm{d}^3 q\, e^{i(\boldsymbol{k}_1 + \boldsymbol{k}_2)\boldsymbol{q}} = (2\pi)^3\, \delta(\boldsymbol{k}_1 + \boldsymbol{k}_2)$

where

$$n_\alpha := \omega_\alpha * n \tag{18}$$

To rephrase it transparently: in the low density limit, the ω_α serve as convolution kernels, *i.e. as weights*, so as to get quantities n_α to write the excess free energy low density limit as an expression quadratic in the $\{n_\alpha\}$. The n_α are accordingly referred to as weighted densities.

The weight functions proportional to $\delta(R-r)$ all sample the particle density on the surface of a sphere; the differing prefactors are enlightened somewhat in the case of a homogeneous fluid (meaning $\nabla n \equiv 0$), often referred to as the *bulk fluid*, in which case n can be pulled from the convolution such that $n_\alpha = n \cdot \int \omega_\alpha$:

$$n_0 = n \cdot 1 \qquad n_1 = n \cdot R \qquad n_2 = n \cdot 4\pi R^2 \qquad n_3 = n \cdot \frac{4}{3}\pi R^3 \tag{19}$$

It should be commented, that $n_0 = n$ does not in general give n_0 exactly the same interpretation as the unweighted density. n_0 still remains a quantity telling one about *happenings on the hard sphere surface*[5]. n_3 however, by virtue of remaining a three dimensional integral[6], is a bit different in nature: both its general and its homogeneous form represent the (local) packing fraction of the hard sphere gas, i.e. the fraction of the entire volume occupied by the hard spheres.

It is also worth mentioning, that the vectorial weighted densities vanish for $\nabla n \equiv 0$, since the density weighted normal vectors onto the hard sphere's surface $\boldsymbol{r}/r$ are then distributed perfectly symmetrical, rendering their integral 0. $\boldsymbol{n}_1\boldsymbol{n}_2$ is in fact a measure of local inhomogeneity of the hard sphere system: as is seen from its definition, the direction of $\boldsymbol{n}_2 = 4\pi R \cdot \boldsymbol{n}_1$ can be called the dipole of the sphere surface distribution. The larger that surface distribution dipole, the bigger the $\boldsymbol{n}_\alpha$.

2.2.2 Extrapolation to Higher Density Excess Free Energy for Hard Spheres

What is interesting about the hard sphere low density limit (17), is that the excess free energy appears to have a physically well interpretable spatial

---

[5] n_0's great similarity to n will often result in it playing a similar role as n in thermodynamic expression though

[6] as in: not ground down to surface integrals by the weight functions, as n_0, n_1 and n_2 are

density $\beta F_{\mathrm{ex}} \approx \int \mathrm{d}^3 r\, \Phi(\boldsymbol{r})$ and what is more, that this spatial density is not explicitly position dependent, but a function of the weighted densities, such that the excess free energy is of the form $\beta F_{\mathrm{ex}} \approx \int \mathrm{d}^3 r\, \Phi(\{n_\alpha(\boldsymbol{r})\})$. What Rosenfeld postulated to be approximately valid in [10], is that for higher densities the excess free energy density remained only a function of the weighted densities. Since Φ is of dimension length^{-3} its n_α-dependence cannot look just any way. Of course, the dimensions must match, but furthermore the weighted densities that are not dimensionless shall not appear with negative power as in $n_1 n_1/n_2$, so that the free energy's link to the virial expansion via the pressure equation is not jeopardized [10]. This leaves only the combinations n_0, $n_1 n_2$, $\boldsymbol{n}_1 \boldsymbol{n}_2$, ${n_2}^3$, $n_2 \boldsymbol{n}_2 \boldsymbol{n}_2$. At this stage, the dependence on n_3 can be arbitrary, as long as it is multiplied with a term of the correct dimensions, thus yielding the general Form

$$\Phi = f_1(n_3)\, n_0 + f_2(n_3)\, n_1 n_2 + f_3(n_3)\, \boldsymbol{n}_1 \boldsymbol{n}_2 + f_4(n_3)\, {n_2}^3 + f_5(n_3)\, n_2 \boldsymbol{n}_2 \boldsymbol{n}_2 \quad (20)$$

To reproduce the low density limit (17) it is necessary as $n \to 0$ that $f_1(n_3) \to n_3$, $f_2(n_3) \to 1$, $f_3(n_3) \to -1$ and f_4, f_5 to approach negligible constants. This is to be expected of the latter two terms, whose order in particle number density is n^3 , making them quantifiers of multi-particle, meaning more than three-particle, interactions.

The quality of extrapolation now seems to rely on the quality of physical information poured into the coefficients. [10], [11], [4] have related the pressure equation[7] of the homogeneous fluid

$$\beta p = n - \Phi + \sum_\alpha \frac{\partial \Phi}{\partial n_\alpha} n_\alpha \quad (21)$$

to some other known pressure expression. Rosenfeld, for example argued that $\beta p = \partial \Phi / \partial n_3$ (which will be elaborated upon later, when it becomes relevant) to render five uncoupled differential equations (two pairs of them being the same, reducing the calculus to three equations). The up to order n^2 integration constants are predetermined by the low density limit. He then used knowledge of the third virial coefficient for fixing the n^3-order

---

[7] The pressure equation takes this form, because $\beta p_{\mathrm{id}} = n$ and $\partial n_\alpha / \partial V = -n_\alpha / V$, which can be used in the following way: $\beta p = -\beta \frac{\partial F}{\partial V} = n - \frac{\partial}{\partial V}(V\Phi) = n - \Phi - V \sum_\alpha \frac{\partial n_\alpha}{\partial V} \frac{\partial \Phi}{\partial n_\alpha} = n_0 - \Phi + \sum_\alpha \frac{\partial \Phi}{\partial n_\alpha} n_\alpha$

integration constants [10] to arrive at

$$\begin{aligned}\Phi_{\mathrm{RF}} &= n_0 \log\left(\frac{1}{1-n_3}\right) + \\ &(n_1 n_2 - \boldsymbol{n}_1 \boldsymbol{n}_2)\left(\frac{1}{1-n_3}\right) + \\ &(n_2 n_2 n_2 - 3\, n_2 \boldsymbol{n}_2 \boldsymbol{n}_2)\,\frac{1}{24\pi}\left(\frac{1}{1-n_3}\right)^2\end{aligned} \tag{22}$$

which demonstrates the feasibility of this approach and performs well at comparatively low packing fractions, but fails to predict the entropically driven crystallization of the hard sphere gas observed at higher packing fractions, as Rosenfeld points out later in the same paper [10].

The most powerful Fundamental Measure Theory free energy density function found thus far is **White Bear II** [4], in the following denoted Φ_{WB}, which was derived by using a generalization of the empirical, but performant Carnahan-Starling [3] equation of state (of the hard sphere gas), which when formulated in terms of the $\{n_\alpha\}$ reads [4]

$$\begin{aligned}\beta p &= n_0\left(\frac{1}{1-n_3}\right) + \\ &n_1 n_2\left(\frac{1}{1-n_3}\right)^2 \cdot \left(1-\frac{1}{3}n_3\right) + \\ &{n_2}^3\,\frac{1}{12\pi}\left(\frac{1}{1-n_3}\right)^3 \cdot \left(1-\frac{2}{3}+\frac{1}{3}{n_3}^2\right)\end{aligned} \tag{23}$$

Rosenfelds functional when inserted into the pressure equation yields a less accurate equation of state

$$\beta p = n_0\left(\frac{1}{1-n_3}\right) + n_1 n_2\left(\frac{1}{1-n_3}\right)^2 + {n_2}^3\,\frac{1}{12\pi}\left(\frac{1}{1-n_3}\right)^3 \tag{24}$$

which happens to be the same as the equation of state derived from the Percus-Yervick equation[8] [4]. The difference between Φ_{WB} and Φ_{RF} is that

---

[8] The Percus-Yervick equation is the Ornstein-Zernike equation under Percus-Yervick approximation; this statement is enlightened in the section on the direct correlation function later on

the Rosenfeld-($n_1 n_2 - \boldsymbol{n}_1 \boldsymbol{n}_2$)-term is multiplied by another n_3-dependent quantity $\tilde{f}_2(n_3)$ given by

$$\tilde{f}_2(n_3) := 1 + \frac{1}{3}\left(2 - n_3 - 2\left(\frac{n_3}{1-n_3}\right)^{-1}\log\left(\frac{1}{1-n_3}\right)\right) \tag{25}$$

and the Rosenfeld-(${n_2}^3 - 3\, n_2 \boldsymbol{n}_2 \boldsymbol{n}_2$)-Term by $\tilde{f}_4(n_3)$

$$\tilde{f}_4(n_3) := 1 - \frac{1}{3}\left(\frac{2 - 3n_3 + 2{n_3}^2}{n_3}\right) + \frac{2}{3}\left(\frac{n_3}{1-n_3}\right)^{-2}\log\left(\frac{1}{1-n_3}\right) \tag{26}$$

Both the $\tilde{f}_j$ factors have an expansion $1 + \mathcal{O}(n_3)$, so for low packing fractions Φ_{RF} is recovered. In contrast to Φ_{RF}, Φ_{WB} predicts the crystallization at high packing fractions [4].

2.3 Results from the Theory of Fluids

2.3.1 The Direct Correlation Function

The particle number density is only one function in a class of functions describing system structure, the so called l-particle distribution functions

$$n_l(\boldsymbol{r}_1, \ldots, \boldsymbol{r}_l) := \frac{N!}{(N-l)!}\,\langle\, \delta(\boldsymbol{x}_1 - \boldsymbol{r}_1) \cdots \delta(\boldsymbol{x}_l - \boldsymbol{r}_l)\,\rangle \tag{27}$$

which are the probability of finding l particles in exactly the places passed to n_l, no matter what the positions of the remaining $N - l$ particles might be [5].

The one of interest here is the two particle distribution function $n_2(\boldsymbol{r}, \boldsymbol{q})$, because it contains information about how many particle pairs are within interaction distance of each other and thus of the energy bound up in particle interactions. If the particle positions were uncorrelated, $n_2(\boldsymbol{r}, \boldsymbol{q})$ would just factor into $n(\boldsymbol{r}) \cdot n(\boldsymbol{q})$. The degree to which it does not is measured by a function $g(\boldsymbol{r}, \boldsymbol{q})$ [5]

$$n_2(\boldsymbol{r}, \boldsymbol{q}) =: n(\boldsymbol{r})\, n(\boldsymbol{q})\, g(\boldsymbol{r}, \boldsymbol{q}) \tag{28}$$

If g is a function of $|\boldsymbol{r} - \boldsymbol{q}|$ only, it is referred to as the *radial distribution function*, since for an arbitrary origin $n \cdot 4\pi r^2\, \mathrm{d}r\, g(r)$ counts the number of particles found in a shell of volume $4\pi r^2\, \mathrm{d}r$ at radius r around said origin.

For the ideal gas $g_{\mathrm{id}} \equiv 1$. The correlation between $\boldsymbol{r}$ and $\boldsymbol{q}$ motivates the definition of the structure function $h(r) := g(r) - 1$

$$\frac{n_2(\boldsymbol{r}, \boldsymbol{q}) - n(\boldsymbol{r})\, n(\boldsymbol{q})}{n(\boldsymbol{r})\, n(\boldsymbol{q})} = (g(\boldsymbol{r}, \boldsymbol{q}) - 1)$$

where e.g. for the ideal gas h_{id} vanishes. Ideal gases are in that sense featureless. Given the the concept of the radial distribution function, Ornstein and Zernike for homogeneous fluids defined the *direct correlation function* $c(r)$ via the integral equation [8]

$$h(|\boldsymbol{r}|) = c(|\boldsymbol{r}|) + n \cdot h * c\,(\boldsymbol{r}) = c + n \int \mathrm{d}^3 q\, h(|\boldsymbol{q}|) c(|\boldsymbol{r} - \boldsymbol{q}|) \tag{29}$$

which can be thought of as a split into short range correlations given by c and longer range correlations given by the rest [8]. As for the ideal gas $h_{\mathrm{id}}(r) = 0$, the Ornstein-Zernike equation becomes $c = 0$, showing that non-vanishing $c(r)$ is due to interactions. It can in fact be shown [11] that, in the context of Classical Density Functional theory applied to homogeneous systems, $c(r)$ is related to the excess free energy by

$$c(|\boldsymbol{r} - \boldsymbol{q}|) = -\frac{\delta^2\, \beta F_{\mathrm{ex}}}{\delta n(\boldsymbol{r})\, \delta n(\boldsymbol{q})}[n_{\mathrm{eq}}] \tag{30}$$

For dilute gases, g can be approximated by the Boltzmann factor of a two pair particle interaction

$$g(r) \overset{n \to 0}{\approx} e^{-\beta u(r)} \tag{31}$$

but for higher densities k-particle correlations modify the g expression for the dilute limit by the so called cavity distribution function $y(r)$

$$g(r) =: e^{-\beta u(r)}\, y(r) \tag{32}$$

which, if its n-dependence is expanded in powers of n, has the interpretation of contributions to $g(r)$ by $(l + 2)$-particle interactions [7].

2.3.2 Barker-Henderson Effective Hard Sphere Diameter [1]

Barker-Henderson perturbation theory is a framework for describing softly interacting systems as perturbations upon the hard sphere gas, *assuming they effectively rise to infinity for small interaction distances* r. The perturbation is set up as follows: first, an interaction distance d is introduced, in order to establish what "small" means. Next, an interaction distance $d < \sigma$ is picked, that divides the potential into sections considered repulsive for $r < \sigma$ and attractive for $r > \sigma$ respectively. Then then the following effective interaction potential is defined

$$u_{\text{eff}}(r) = \begin{cases} u(d + (r-d)/\alpha) & r < ((1-\alpha)d + \alpha\,\sigma) \\ 0 & ((1-\alpha)d + \alpha\,\sigma) < r < \sigma \\ \gamma \cdot u(r) & \sigma < r \end{cases} \tag{33}$$

This warrants some elaboration: $u_{\text{eff}}(0)$ has the value $u(d(1-1/\alpha))$ and then interpolates between $u(d(1-1/\alpha))$ and $u((1-\alpha)d + \alpha\sigma)$ up until r reaches $(1-\alpha)d + \alpha$. α does two things simultaneously. For one it determines the steepness of the repulsive part of the potential. Then, also it determines the width of the remaining gap, in which the potential can be considered to vanish before taking on the γ-attenuated value $u(r)$ again, $\alpha = 1$ closing that gap and $\alpha \to 0$ making it go all the way to d.

$\alpha = \gamma = 0$, so long as the values of u at $r < d$ indeed are effectively infinite, one retrieves the hard sphere potential with d as the hard sphere diameter. For $\alpha = \gamma = 1$ the original potential comes out. Barker-Henderson perturbation consists of Taylor-expanding the excess-term in $\log Z = \log(Z_{\text{id}} Z_{\text{ex}}) = \log Z_{\text{id}} + \log Z_{\text{ex}}$[9] around $(\alpha, \gamma) = 0$ assuming not u, but u_{eff} is the interaction potential.

When doing that to first order, one arrives at

$$\begin{aligned} -\log Z_{\text{ex}} =& \beta F_{\text{ex,h}} \\ & + n \cdot 2\pi d^2\, g_{\text{h}}(d) \cdot \left(d - \int_0^\sigma \mathrm{d}r\ \left(1 - e^{-\beta u(r)}\right) \right) \cdot \alpha \\ & + \gamma \text{ dependence and higher orders in } \alpha \end{aligned}$$

where $F_{\text{ex,h}}$ is the hard-sphere excess free energy and g_{h} the hard sphere radial distribution function. Choosing

$$d = \int_0^\sigma \mathrm{d}r\ \left(1 - e^{-\beta u(r)}\right) \tag{34}$$

---

[9] where Z here denotes is the *canonical* partition function and thus technically is defined for fixed particle number only, in contrast to the rest of the mentionings of Z here. This does not stop one from using the effective radius formula though.

makes the α-dependence vanish in first order. That would have the interpretation of a hard-sphere gas with sphere diameter d being, with respect to the steepness/repulsivity, a good approximation to $u(r)$ already. d from equation 34 can thus with confidence be referred to as an effective hard-sphere diameter.

3 Step Potential Free Energy from Fundamental Measure Theory

To ease the distinction to hard sphere functionals, soft interaction functionals will be denoted with φ instead of Φ. Furthermore, because the factor appears very often,

$$\xi := 1 - e^{-\beta h}$$

is defined and used from here on.

The goal of this section is to find thinkable ways one might approximate step potential free energy within the Fundamental Measure Theory framework. What any approach has to mend, is that the hard sphere gas phase diagram does not have a temperature dependence, all effects are entropic. Energy has to come into play at some point. Two approaches to achieve this will be looked at:

1. Thinking of the step potential to have a temperature dependent effective exclusion volume, modeling that as a hard sphere and *adding the interaction energy onto the resulting entropic hard sphere contribution*

2. *Emulating Rosenfelds original [10] derivation* of the hard sphere Fundamental Measure Theory, but at the stage where excess chemical potential is computed [9] remember that particle insertion comes at an energy cost

3.1 First Approach: Hard Sphere Functionals with Energy Terms

The Barker-Henderson-results [1] demonstrate, that the hard sphere gas can be used as a reference system for soft interactions. Simply modeling them with hard spheres of a temperature dependent effective hard-sphere diameter however, neglects energy stored in step potential interactions. That is because hard spheres just interact with perfectly inelastic collisions. The hard sphere excess over ideal gas free energy is given purely by the entropical effects stemming from the mutual exclusion of particle volumes. The internal energy part of the step potential excess free energy may however very well become non-negligible in non-dilute softly interacting systems. The way stored energy will be accounted for in this approach, is by writing excess over ideal gas internal energy U_{int} in terms of $n(\boldsymbol{r})$, so as to use the expression in Density Functional Theory, and then add that energy expression onto a hard sphere excess free energy term with the Barker-Henderson effective diameter as hard-sphere diameter.

White Bear II with an Effective Hard Sphere Radius As discussed in the section on Barker-Henderson perturbation theory, given a soft interaction, the effective hard sphere diameter d from (34) is the particle diameter of a first order approximation of that interaction by a hard-sphere gas. In the case of the step potential, there is no attractive part, making the Barker-Henderson-σ of choice $\sigma \to \infty$

$$R_{\text{BH}} := \frac{1}{2}\int_0^\infty \mathrm{d}r\, \left(1 - e^{-\beta u(r)}\right) = R(1 - e^{-\beta h}) = R\xi \tag{35}$$

(35) is plotted in fig. 1.

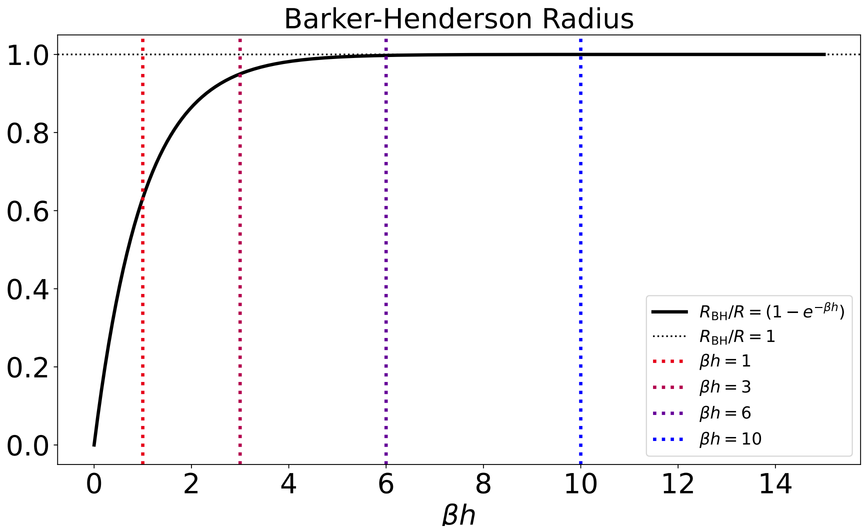

Figure 1: Plot of $R_{\mathrm{BH}}/R = \xi$, because exactly knowing its value for various βh helps checking results. βh-values used often throughout this text are marked as well.

R_{BH} will be used together with the White Bear II functional, by rescaling all weighted densities[10] n_α according to what fundamental measure they belong to:

$$\begin{aligned} n_{0,\mathrm{BH}} &= n_0 \\ n_{1,\mathrm{BH}} &= (R_{\mathrm{BH}}/R) \cdot n_1 \\ n_{2,\mathrm{BH}} &= (R_{\mathrm{BH}}/R)^2 \cdot n_2 \\ \boldsymbol{n}_{1,\mathrm{BH}} &= (R_{\mathrm{BH}}/R) \cdot n_1 \\ \boldsymbol{n}_{2,\mathrm{BH}} &= (R_{\mathrm{BH}}/R)^2 \cdot n_2 \\ n_{3,\mathrm{BH}} &= (R_{\mathrm{BH}}/R)^3 \cdot n_3 \end{aligned} \tag{36}$$

There also would have been the option to instead of reweighting the densities replace the radius, which the weight functions are defined with, by the Barker-Henderson radius. But Monte Carlo simulations (seen e.g. in fig. 9) dissuade that: as is depicted in fig. 2, the radius of the direct correlation

---

[10] in the hard sphere term only, the energy term has nothing to do with this and uses the normal n_α

functions support (which is also the radius at which the $h(r)$ to this $c(r)$ has its discontinuity) for $\beta h = 1, 3$ is then too small.

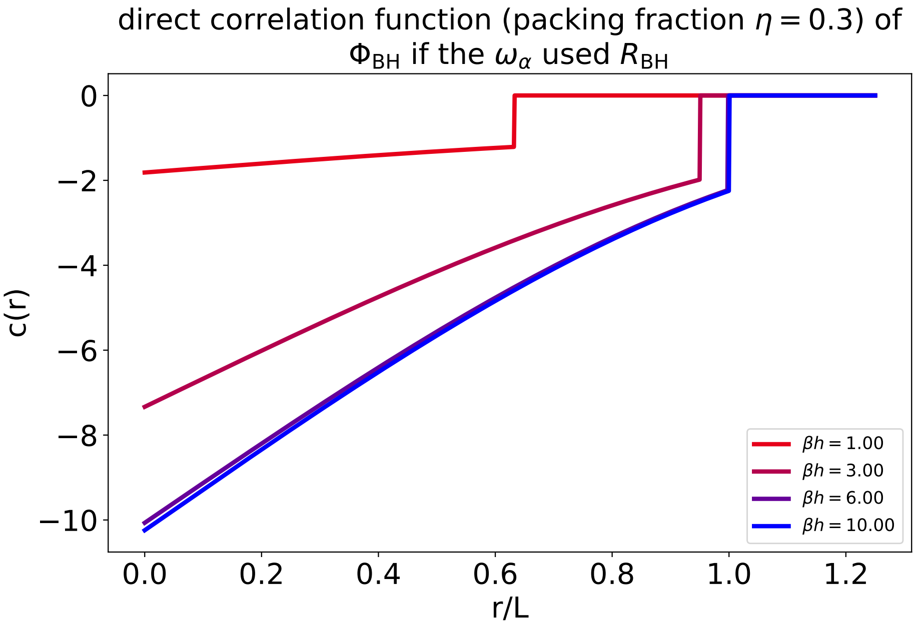

Figure 2: Direct correlation function $c(r)$ for $\beta F_{\mathrm{ex}} \approx \int \Phi_{\mathrm{BH}}$ if the weight functions ω_α used in the n_α were defined with by the Barker-Henderson-Radius R_{BH}. Φ_{BH} is the functional, which is at this is stage being constructed, but without the energy contribution, see equation 43.

Energy Term Excess internal energy U_{int} is given by taking the probability of finding particles at $\boldsymbol{r}$ and $\boldsymbol{q}$ multiplied with the interaction energy $u(|\boldsymbol{r}-\boldsymbol{q}|)$ that entails and integrating it over all combinations of $\boldsymbol{r}$ and $\boldsymbol{q}$ (and a 1/2 correction factor because of double counting)

$$U_{\mathrm{int}} = \frac{1}{2} \int \int \mathrm{d}^3 r \, \mathrm{d}^3 q \; n_2(\boldsymbol{r}, \boldsymbol{q}) \, u(|\boldsymbol{r} - \boldsymbol{q}|) \tag{37}$$

which by (28) and the form of the step potential (48) can be written as

$$U_{\mathrm{int}} = \frac{1}{2} \int \int \mathrm{d}^3 r \, \mathrm{d}^3 q \; n(\boldsymbol{r}) \, n(\boldsymbol{q}) \, g(\boldsymbol{r}, \boldsymbol{q}) \, u(|\boldsymbol{r} - \boldsymbol{q}|) \tag{38}$$

3.1.1 Expressing the Energy Term with Fundamental Measure Theory

Using $n \to 0$ Radial Distribution Approximation How to integrate the energy and hard sphere contributions with each other is not clear from the onset, because the energy term is not formulated in terms of Fundamental Measure Theory. One way to achieve a reformulation, is to have the $\Theta(L-r)$ factor somehow be the only $\boldsymbol{r}$- and $\boldsymbol{q}$-dependent one in the integrand of

$$\beta U_{\text{int}} = \frac{1}{2} \int \int \mathrm{d}^3 r \, \mathrm{d}^3 q \, n(\boldsymbol{r}) n(\boldsymbol{q}) \, g(|\boldsymbol{r} - \boldsymbol{q}|) \, \beta u(|\boldsymbol{r} - \boldsymbol{q}|)$$

from (38), so as to be back in the situation in equation 17. That of course has to be done by approximating the radial distribution function in that manner.

The approximation of choice will be the $n \to 0$ limit of the radial distribution function from (31). Conveniently, now

$$e^{-\beta h \Theta(L-r)} \, \Theta(L-r) = e^{-\beta h} \, \Theta(L-r) \tag{39}$$

can be used. Inserting the assumed distribution function and the step potential $u(r) = h \, \Theta(L-r)$ into the excess internal energy equation (38) results in

$$\beta U_{\text{int}} = e^{-\beta h} \beta h \cdot \frac{1}{2} \int \int \mathrm{d}^3 r \, \mathrm{d}^3 q \, n(\boldsymbol{r}) n(\boldsymbol{q}) \, \Theta(L - |\boldsymbol{r} - \boldsymbol{q}|) \tag{40}$$

Using that $-\Theta(L-r)$ has the decomposition (8) turns (38) into

$$\beta U_{\text{int}} = e^{-\beta h} \beta h \int (n_0 n_3 + n_1 n_2 - \boldsymbol{n}_1 \boldsymbol{n}_2) \tag{41}$$

The excess internal energy density can now be read off (41)

$$\varphi_{\text{int}} = e^{-\beta h} \beta h \cdot (n_0 n_3 + n_1 n_2 - \boldsymbol{n}_1 \boldsymbol{n}_2) \tag{42}$$

Using the pair interaction energy expression (38) to use Fundamental Measure Theory has been done before, e.g. in [2] where Fundamental Measure Theory is appliead to study the classical density functional theory of the square well potential[11].

---

[11] Incidentally, that square well free energy expression also involves Barker-Henderson-Theory, but with the difference, that a free energy expression for the square well is used, that Barker and Henderson derived with their tools from [1]. In φ_{BH}, the energy term does not make any contact with Barker-Henderson theory. Instead, their effective hard sphere diameter (35) is used to model an effective exclusion volume by (36)

Resulting Equation of State Now adding the energy onto the hard sphere contribution to excess free energy, as announced earlier, one arrives at

$$\varphi_{\mathrm{BH}} := \varphi_{\mathrm{int}} + \Phi_{\mathrm{BH}} \tag{43}$$

where the BH subscript denotes, that Φ_{BH} is the White Bear II functional, but with the weighted densities reweighted by the appropriate powers of (R_{BH}/R) (see equation 36). It is important to not forget, that the interaction energy contribution still uses the original radius R, because the effective hard sphere radius in this approach is not thought of as diminishing interaction range, but instead as shrinking the effective exclusion volume resulting from it.

Since φ_{BH} is expressed purely in terms of the Fundamental Measure Theory weighted densities, one can insert it into the pressure equation (21). The hard-sphere contribution to pressure is found to be

$$-\Phi_{\mathrm{BH}} + \sum_\alpha n_\alpha \frac{\partial \Phi_{\mathrm{BH}}}{\partial n_\alpha} = -\Phi_{\mathrm{BH}} + \sum_\alpha n_{\alpha,\mathrm{BH}} \frac{\partial \Phi_{\mathrm{BH}}}{\partial n_{\alpha,\mathrm{BH}}} \tag{44}$$

which will have the same result as White Bear II, just with the $n_{\alpha,\mathrm{BH}}$ instead of the n_α. The sum in the energy contribution is

$$\sum_\alpha n_\alpha \frac{\partial \varphi_{\mathrm{int}}}{\partial n_\alpha} = e^{-\beta h}\beta h(2n_0n_1 + 2n_1n_2 - 2\boldsymbol{n}_1\boldsymbol{n}_2) = 2\varphi_{\mathrm{int}} \tag{45}$$

Thus

$$\begin{aligned} \beta p &= \left(n_0 - \Phi_{\mathrm{BH}} + \sum_\alpha n_\alpha \frac{\partial \Phi_{\mathrm{BH}}}{\partial n_\alpha}\right) - \varphi_{\mathrm{int}} + \sum_\alpha n_\alpha \frac{\partial \varphi_{\mathrm{int}}}{\partial n_\alpha} \\ &= \left(n_0 - \Phi_{\mathrm{BH}} + \sum_\alpha n_\alpha \frac{\partial \Phi_{\mathrm{BH}}}{\partial n_\alpha}\right) + \varphi_{\mathrm{int}} \end{aligned} \tag{46}$$

which after setting the vectorial densities to 0 (because the bulk fluid is considered) reads

$$\begin{aligned} \beta p \ &= \ e^{-\beta h}\beta h \cdot (n_0n_3 + n_1n_2) \\ &\quad + \frac{n_0}{1-\xi^3 n_3} \\ &\quad + \frac{\xi n_1 \cdot \xi^2 n_2}{(1-\xi^3 n_3)^2} \cdot \left(1 + \frac{1}{3}\left(\xi^3 n_3\right)^2\right) \\ &\quad + \frac{\xi^2 n_2 \cdot \xi^2 n_2 \cdot \xi^2 n_2}{12\pi(1-\xi^3 n_3)^3} \cdot \left(1 - \frac{2}{3}\xi^3 n_3 + \frac{1}{3}\left(\xi^3 n_3\right)^2\right) \end{aligned} \tag{47}$$

On Barriers to Using Higher Orders of the $y(r)$ Expansion Using the approximation $g(r) \approx e^{-\beta h}$ for computing the energy term means, that only the 0^{th} order of the expansion of $y(r)$ in powers of n has been considered. One can ask, what happens if more orders were included. Because e.g. $y_1 = f * f$ [7] which is *not* proportional to $\Theta(L - r)$ (nor is it even an indicator function), one cannot make use of (8) anymore. That barrier to applying Rosenfeld's Mayer-f decomposition of course persists for all higher orders of $y(r)$. However, proposing that the excess internal energy density from (41) is the low density limit of a more generally valid *function* of the n_α (just as Rosenfeld did), might render results. However, additional information is still necessary in order to write down an expression (e.g. Rosenfeld needed information about the third virial coefficient).

3.2 Second Approach: Particle Insertion Work

The Mayer-f function of the step potential

$$u_{\mathrm{s}}(r) := h\,\Theta(L-r) \tag{48}$$

(where L is the distance at which a force acts, very analogous to the hard sphere diameter) reads

$$f_{\mathrm{s}}(r) = e^{-\beta u_{\mathrm{s}}} - 1 = \left(e^{-\beta h} - 1\right)\,\Theta(L-r) \tag{49}$$

Just as the hard sphere gas Mayer-f function, one can decompose $\Theta(L-r)$ according to (8) and write down the low density limit expansion of this model in terms of Fundamental Measure Theory's weighted densities

$$\begin{aligned}\beta F_{\mathrm{ex}}[n] &\overset{n\to 0}{\approx} \left(1-e^{-\beta h}\right)\int (n_0 n_3 + n_1 n_2 - \boldsymbol{n}_1 \boldsymbol{n}_2)\\ &= \int \xi(n_0 n_3 + n_1 n_2 - \boldsymbol{n}_1 \boldsymbol{n}_2)\end{aligned} \tag{50}$$

where $R := L/2$ is the radius used to define the n_α.

One can now ask, whether it works out to enforce this low density limit and try to proceed to extrapolate this to higher densities in the manner Rosenfeld did. At this stage the differences to the hard sphere gas come into play: the presence of "sphere overlaps" (as in, spheres close in below L) and the associated overlap energy.

3.2.1 Emulating Rosenfeld's Extrapolation Approach for the Step Potential

When Rosenfeld derived the hard sphere functional's extrapolation to higher densities, he imposed $\beta p = \partial\Phi/\partial n_3$. That relation comes from the idea, that the excess over ideal gas chemical potential μ_{ex} of any system is exactly the reversible work necessary to insert another particle. Since they cannot overlap, for hard spheres this is the smallest amount of work W necessary to create a cavity able to hold the inserted particle, which can be shown [9] to have of the form

$$W = p\cdot\left(\frac{4}{3}\pi R^3\right) + \cdots \tag{51}$$

where p is the pressure and the dots denote terms unimportant to the discussion. Going back to the excess free energy density, in the homogeneous case, thermodynamics shows

$$\beta\mu_{\text{ex}} = \frac{\partial\,\beta F_{\text{ex}}}{\partial N} = \frac{\partial\Phi}{\partial n} = \sum_{\alpha} \frac{\partial\Phi}{\partial n_\alpha}\frac{\partial n_\alpha}{\partial n}$$

$$= \frac{\partial\Phi}{\partial n_3}\cdot\left(\frac{4}{3}\pi R^3\right) \;+\; \frac{\partial\Phi}{\partial n_2}\cdot\left(4\pi R^2\right) \;+\; \frac{\partial\Phi}{\partial n_1}\cdot R \;+\; \frac{\partial\Phi}{\partial n_0}\cdot 1 \tag{52}$$

Comparing (51) and (52) via $W = \mu_{\text{ex}}$ allows to see the analogy in the expressions and to conclude that indeed $\partial\Phi/\partial n_3$ is βp[12] [11]. When trying to do the same for the step potential there is a complication though: to insert the particle it is not necessary to create a cavity of diameter L, as overlaps are allowed, even if they come at an internal energy cost.

Estimating the $u(r)$-Contribution to Insertion Work The effect of this is, that the cavity necessary to insert another particle with minimal reversible work necessary might have a smaller radius $R' < R$. It will turn out, that thinking about the value of R' at this stage is unnecessary (equation 64). Going forward it will merely be used, that it is the smallest distance that the centers of system particles can close in at the center of the cavity. Let $d(\boldsymbol{r})$ be the thermal equilibrium distribution of particles outside the cavity. For a small, spherical cavity, d should be radially symmetric and look very similar to $g(r)$.

Because overlaps are allowed, in contrast to the hard sphere gas, the insert particle is, in principle, not necessarily in the center. So the reversible insertion work contribution W_{int} stemming from the external potential v_{sys}, which the system causes the insert particle to experience, is given by

$$e^{-\beta W_{\text{int}}} = \int_{\text{cavity}} \frac{\mathrm{d}^3 r}{4\pi R'^3/3}\, e^{-\beta v_{\text{sys}}(\boldsymbol{r})} \tag{53}$$

Introducing another approximation, that v_{sys} is constant within the cavity

$$\int_{\text{cavity}} \frac{\mathrm{d}^3 r}{4\pi R'^3/3}\, e^{-\beta v_{\text{sys}}(\boldsymbol{r})} \approx e^{-\beta v_{\text{sys}}(0)} \tag{54}$$

---

[12] For general shapes area, volume and length are not related and can thus change independently from each other. They just happen to be related for spheres. What $\partial\Phi/\partial n_3 = \beta p$ expresses, is that pressure is essentially the ratio $\delta\Phi/\delta V$ of a change $\delta\Phi$ in Φ to the change in cavity volume δV that caused $\delta\Phi$ in the first place, while all other fundamental measures are kept fixed.

allows identifiying $v_{\text{sys}}(0)$ with W_{int}

$$W_{\text{int}} \approx v_{\text{sys}}(0) = n \int_{R'}^{\infty} 4\pi r^2 \, \mathrm{d}r \, d(r) \, u(r) \tag{55}$$

where in the integral to the very right of (55) the contribution of every part within the system to the external potential's value at the cavity center $r = 0$ is collected.

Integrating Insertion Work with Fundamental Measure Theory Adding the expression for the $u(r)$-caused reversible insertion work onto the volume contribution to cavity creation work $p \cdot 4\pi R'^3/3$ now is the

$$W = \left(p \left(\frac{R'}{R} \right)^3 + \frac{W_{\text{int}}}{\frac{4}{3}\pi R^3} \right) \left(\frac{4}{3}\pi R^3 \right) + \cdots \tag{56}$$

where once again the dots stand for terms associated with other fundamental measures and thus of no relevance for $\partial\varphi/\partial n_3$. Now equating $\beta\mu_{\text{ex}} = \frac{\partial\varphi}{\partial n_3} \left(\frac{4}{3}\pi R^3 \right) + \cdots$ with βW and comparing coefficients results in

$$\frac{\partial\varphi}{\partial n_3} = \beta p \left(\frac{R'}{R} \right)^3 + \frac{\beta W_{\text{int}}}{\frac{4}{3}\pi R^3} \tag{57}$$

It will turn out to ease solving the equation to define $\tilde{n}_3 := (R'/R)^3 n_3$. Because R' is n-dependent though, and Rosenfeld used n_0 and n interchangeably in thermodynamic relations, it has to be ensured that handling n_0 in a similar way in the present case is fine. Doing this is as legitimate as Fundamental Measure Theory is, because *by assumption* φ has no explicit n-dependence, but a value for n has to be passed.

Proceeding, by cleaning up expressions by defining the dimensionless

$$\begin{aligned} \lambda &:= \frac{\beta W_{\text{int}}}{(4\pi R'^3/3)\, n_0} \\ &= \int_{R'}^{\infty} \frac{4\pi r^2 \, \mathrm{d}r}{4\pi R'^3/3} \, d(r) \, \beta u(r) \\ &= 3 \int_1^{\infty} \mathrm{d}s \, s^2 \, d(sR') \, \beta u(sR') \end{aligned} \tag{58}$$

yields the equation

$$\frac{\partial\varphi}{\partial\tilde{n}_3} = \beta p + n_0 \lambda \tag{59}$$

Solving the Equation 59 βp is given by φ's pressure equation (21). Inserting that into (57) and pulling

$$n_3 \frac{\partial \varphi}{\partial n_3} = \tilde{n}_3 \frac{\partial \varphi}{\partial \tilde{n}_3} \tag{60}$$

to the left-hand side of the equation results in

$$(1 - \tilde{n}_3) \frac{\partial \varphi}{\partial \tilde{n}_3} = (1 + \lambda) n_0 - \varphi + \sum_{\alpha \neq 3} n_\alpha \frac{\partial \varphi}{\partial n_\alpha} \tag{61}$$

This suggests the next steps: inserting Rosenfelds ansatz (20) a separation of variables argument completely analogous to [10] (enabled by λ being explicitly only dependent on n_0 and temperature) renders five uncoupled differential equations for all of the f_j. The equation for f_1 reads

$$(1 - \tilde{n}_3) \frac{\partial f_1}{\partial \tilde{n}_3} = 1 + \lambda \tag{62}$$

This equation is solved by

$$f_1 = (1 + \lambda) \log \left(\frac{1}{1 - \tilde{n}_3} \right) + f_1(0) \tag{63}$$

where the integration constant is forced to $f_1(0) = 0$ by the the low density limit (50) $f_1 = \xi \left(0 + n_3 + \mathcal{O}\left({n_3}^2\right)\right)$. The expansion also gives information about the first order of f_1 in n_3 and thus, by inserting the definition of $\tilde{n}_3$ and comparing coefficients, enforces a compatibility condition on λ and R'

$$R'^3 (1 + \lambda) = R^3 \xi \tag{64}$$

To get closed expressions for λ and R', one of them has to be known exactly or an approximation has to serve as a second equation for solution. Continuing with f_2 and f_3, they both have the same differential equation

$$(1 - \tilde{n}_3) \frac{\partial f_j}{\partial \tilde{n}_3} = f_j \tag{65}$$

but different low-density-limit-imposed initial conditions $f_2 = \xi + \mathcal{O}(n_3)$ and $f_3 = -\xi + \mathcal{O}(n_3)$, that fix the integration constant of the solution $f_j = f_j(0) \left(\frac{1}{1 - \tilde{n}_3} \right) = f_j(0) \left(1 + \mathcal{O}(n_3)\right)$, resulting in

$$f_2 = \xi \cdot \left(\frac{1}{1 - \tilde{n}_3} \right) \tag{66}$$

$$f_3 = -\xi \cdot \left(\frac{1}{1-\tilde{n}_3}\right) \tag{67}$$

The equations for f_4 and f_5 are

$$(1-\tilde{n}_3)\,\frac{\partial f_j}{\partial \tilde{n}_3} = 2\,f_j \tag{68}$$

which are solved by

$$f_i = f_i(0)\left(\frac{1}{1-\tilde{n}_3}\right)^2 = f_i(0)\,(1+\mathcal{O}\,(n_3)) \tag{69}$$

Finding $f_4(0)$ and $f_5(0)$ requires information beyond second order in density, the third virial coefficient. That computation is done in the appendix (sec. B) and yields the results

$$f_5(0) = -3\,f_4(0) \tag{70}$$

$$f_4(0) = \frac{1}{24\pi}\cdot\frac{1}{3}\left(10\xi^3 - \frac{\xi}{1+\lambda_0}\left(\xi + \frac{3\cdot\lambda_1}{R^3}+6\right)\right) \tag{71}$$

where λ_0 and λ_1 are the first two coefficients of the n-expansion of λ (83). That expansion is elaborated upon in sec. 3.2.3. The values of λ_0 and λ_1 of course depends on the approximation employed for λ. That too is discussed in sec. 3.2.3.

Inserting all results, φ, assuming some approximation for λ (and by extension for R'), reads

$$\begin{aligned}\varphi \;=\; & (1+\lambda)\cdot n_0 \log\left(\frac{1}{1-\tilde{n}_3}\right) \\ & + \xi\cdot(n_1 n_2 - \boldsymbol{n}_1\boldsymbol{n}_2)\left(\frac{1}{1-\tilde{n}_3}\right) \\ & + \frac{1}{3}\left(10\xi^3 - \frac{\xi}{1+\lambda_0}\left(\xi+\frac{3\cdot\lambda_1}{R^3}+6\right)\right)\cdot(n_2n_2n_2 - 3\,n_2\boldsymbol{n}_2\boldsymbol{n}_2)\,\frac{1}{24\pi}\left(\frac{1}{1-\tilde{n}_3}\right)^2\end{aligned} \tag{72}$$

Inserting this into (59) results in the following equation of state

$$\begin{aligned}\beta p = & \frac{n_0 + n_0\tilde{n}_3\lambda}{1-\tilde{n}_3} \\ & + \xi\cdot\frac{n_1n_2}{(1-\tilde{n}_3)^2} \\ & + \frac{1}{3}\left(10\xi^3 - \frac{\xi}{1+\lambda_0}\left(\xi+\frac{3\cdot\lambda_1}{R^3}+6\right)\right)\cdot\frac{n_2n_2n_2}{12\pi\,(1-\tilde{n}_3)^3}\end{aligned} \tag{73}$$

It will be shown in sec. 3.2.3, that the ideal gas and hard sphere limiting cases are reproduced by this functional

$$\begin{aligned}\lim_{\beta h \to +\infty} \varphi &= \Phi_{\mathrm{RF}} \\ \lim_{\beta h \to 0} \varphi &= 0\end{aligned} \tag{74}$$

3.2.2 Emulating White Bear Functional Derivations for the Step Potential

The White Bear functionals [11], [4] in contrast to [10] sacrifice consistency of their thermodynamics with scaled particle theory [9] for higher thermodynamic accuracy. They do that, by not assuming $\partial\Phi/\partial n_3 = \beta p$ and instead imposing an equation of state. The equation of state derivable from Φ_{RF} is

$$\beta p_{\mathrm{RF}} = \frac{n_0}{1-n_3} + \frac{n_1 n_2}{(1-n_3)^2} + \frac{n_2 n_2 n_2}{12\pi\,(1-n_3)^3} \tag{75}$$

and the equations of state imposed by the White Bear functionals can be thought of as correcting extensions to it, that try to fit first of all to the Carnahan-Starling equation. The one used by Φ_{WB} is

$$\begin{aligned}\beta p_{\mathrm{WB}} \;=\; & \frac{n_0}{1-n_3} \\ & + \frac{n_1 n_2}{(1-n_3)^2} \cdot \left(1 + \frac{1}{3}{n_3}^2\right) \\ & + \frac{n_2 n_2 n_2}{12\pi(1-n_3)^3} \cdot \left(1 - \frac{2}{3}n_3 + \frac{1}{3}{n_3}^2\right)\end{aligned}$$

The equation of state (73) unsurprisingly looks similar to βp_{RF} (and has it as its low temperature limit). This immediately raises the question, if it too can be extended to fit a soft particle equation of state. In the hard sphere limit $\beta h \to \infty$ the pressure from (73) naturally suffers from the same problem as the equation of state derived by Rosenfeld (75), namely an overestimation of the pressure compared to the Carnahan-Starling pressure at higher densities [4]. Unsurprisingly, this particular issue is fixed by making modifications to (73) that emulate the ones done by the White Bear II equation of state relative to (75): multiplying the $n_1 n_2$-term by $(1 + \frac{1}{3}\tilde{n}_3^2)$ and the ${n_2}^3$-term by

$(1 - \frac{2}{3}\tilde{n}_3 + \frac{1}{3}\tilde{n}_3^2)$

$$\begin{aligned}\beta p \;=\; & \frac{n_0 + n_0 \tilde{n}_3 \lambda}{1 - \tilde{n}_3} \\ & + \frac{n_1 n_2}{(1-\tilde{n}_3)^2} \cdot \xi \cdot \left(1 + \frac{1}{3}\tilde{n}_3^2\right) \\ & + \frac{n_2 n_2 n_2}{12\pi(1-\tilde{n}_3)^3} \cdot \frac{1}{3}\left(10\xi^3 - \frac{\xi}{1+\lambda_0}\left(\xi + \frac{3\cdot\lambda_1}{R^3} + 6\right)\right) \cdot \left(1 - \frac{2}{3}\tilde{n}_3 + \frac{1}{3}\tilde{n}_3^2\right)\end{aligned} \tag{76}$$

Equating this with the pressure equation for the general Rosenfeld-ansatz[13] yields three uncoupled differential equations. The first equation reads

$$\tilde{n}_3 \frac{\partial f_1}{\partial \tilde{n}_3} + 1 = \frac{1 + \tilde{n}_3 \lambda}{1 - \tilde{n}_3} \tag{77}$$

which can be separated into $\partial f_1 / \partial \tilde{n}_3 = (1+\lambda)/(1-\tilde{n}_3)$, which with the boundary conditions $f_1 = 1 + \tilde{n}_3 + \mathcal{O}\left(\tilde{n}_3^2\right)$ results in

$$f_1 = (1+\lambda)\,\log\left(\frac{1}{1-\tilde{n}_3}\right) \tag{78}$$

The other two equations are

$$\tilde{n}_3 \frac{\partial f_2}{\partial \tilde{n}_3} + f_2 = \frac{\xi}{(1-\tilde{n}_3)^2} \cdot \left(1 + \frac{1}{3}\tilde{n}_3^2\right) \tag{79}$$

and

$$\begin{aligned}\tilde{n}_3 \frac{\partial f_4}{\partial \tilde{n}_3} + 2 \cdot f_4 = & \frac{1}{3}\left(10\xi^3 - \frac{\xi}{1+\lambda_0}\left(\xi + \frac{3\cdot\lambda_1}{R^3} + 6\right)\right) \\ & \times \frac{1}{12\pi(1-\tilde{n}_3)^3}\left(1 - \frac{2}{3}\tilde{n}_3 + \frac{1}{3}\tilde{n}_3^2\right)\end{aligned} \tag{80}$$

These can be turned into exactly the same equations as for deriving the White Bear II functional by dividing by ξ and $\frac{1}{3}\left(10\xi^3 - \frac{\xi}{1+\lambda_0}\left(\xi + \frac{3\cdot\lambda_1}{R^3} + 6\right)\right)$

---

[13] $f_5 = -3\,f_4$ is already assumed at this point. In the discussion accompanying the incorporation of the third virial coefficient into the derivation of φ_{PIW} (appendix B) it is explained in detail, why that is true

respectively, effectively rescaling the f_j. The result thus is

$$\begin{aligned} f_1 &= (1+\lambda)\cdot f_1^{\mathrm{WB}} \\ f_2 &= \xi \cdot f_2^{\mathrm{WB}} \\ f_4 &= \frac{1}{3}\left(10\xi^3 - \frac{\xi}{1+\lambda_0}\left(\xi + \frac{3\cdot\lambda_1}{R^3} + 6\right)\right)\cdot f_4^{\mathrm{WB}} \end{aligned} \tag{81}$$

where $\tilde{n}_3$ is inserted everywhere instead of n_3. The functional thus defined will from now on be referred to as φ_{PIW} the subscript referencing the "particle-insertion-work" argument at the onset of this derivation.

3.2.3 Notes on R' and λ

Number Density Expansion of λ The expansion of the cavity distribution function $y(r)$ [7] in powers of number density translates in just such an expansion of λ, if assuming

$$d(r) \approx g(r) = e^{-\beta u(r)}\left(1 + n\cdot y_1(r) + n^2\cdot y_2(r) + \cdots\right) \tag{82}$$

For that, one simply has to insert the expansion

$$\begin{aligned} \lambda &= \int_{R'}^{\infty} \frac{4\pi r^2\,\mathrm{d}r}{4\pi R'^3/3}\, e^{-\beta u(r)}\left(1 + n\cdot y_1(r) + n^2\cdot y_2(r) + \cdots\right)\,\beta u(r) \\ &= \lambda_0 + n\,\lambda_1 + n^2\,\lambda_2 + \cdots \end{aligned} \tag{83}$$

where

$$\lambda_k := \int_{R'}^{\infty} \frac{4\pi r^2\,\mathrm{d}r}{4\pi R'^3/3}\, e^{-\beta u(r)}\,\beta u(r)\cdot y_k(r) \tag{84}$$

with $y_0 \equiv 1$ and the appearing factors of n have to be replaced by n_0 before the expression can be used within Fundamental Measure Theory. Because

$$e^{-\beta h\Theta(L-r)}\Theta(L-r) = e^{-\beta h}\,\Theta(L-r) \tag{85}$$

one can write more concretely

$$\lambda_k = e^{-\beta h}\,\beta h\cdot \int_{R'}^{L} \frac{4\pi r^2\,\mathrm{d}r}{4\pi R'^3/3}\, y_k(r) \tag{86}$$

Hard Sphere and Ideal Gas Limit The compatibility condition (64) ensures the following properties

1. *Reproduction of the ideal gas limit.* In the limit $\beta h \to 0$, the factor ξ converges to 0. Equation 64 then forces
$$R'^3(1+\lambda) = R^3\xi \to 0 \tag{87}$$
which causes $\tilde{n_3} = (R'/R)^3\, n_3 \to 0$ and thus $\varphi_{\mathrm{PIW}} \to 0$ so that only the ideal gas contribution to free energy remains.

2. *Reproduction of the hard sphere limit.* In the limit $\beta h \to +\infty$, the factor $\xi \to 1$, such that
$$R'^3(1+\lambda) = R^3\xi \to R^3 \tag{88}$$
To argue, that the hard sphere limit is reproduced, one can use that for all densities and temperatures $d(r) \approx g(r) = e^{-\beta u(r)}\, y(r)$, where the cavity distribution function $y(r)$ contains all number density dependence of g. Combining this with the expression (58) for λ
$$\begin{aligned}\lambda &= 3\int_1^\infty \mathrm{d}s\, s^2\, e^{-\beta h\,\Theta(L-sR')}\,\beta h\,\Theta(L-sR')\,y(sR') \\ &= 3\,e^{-\beta h}\beta h \cdot \frac{1}{R'^3}\int_{R'}^{L}\mathrm{d}r\, r^2\, y(r)\end{aligned} \tag{89}$$
Multiplying by R'^3 allows using the compatibility condition (88) in the form $R'^3\lambda = R^3 - R'^3$
$$R^3 - R'^3 = 3e^{-\beta h}\beta h\left(\int_{R'}^{L}\mathrm{d}r\, r^2\, y(r)\right) \to 0 \tag{90}$$
where one the convergence of (90) is only guaranteed, if R' does not make the integral expression diverge faster that $e^{\beta h}$; it at first seems odd to even conceive of the possibility and ideally $0 < R' < R$. At this stage the appearance of negative R' encountered in the approximation $\lambda \approx \lambda_0$ should be mentioned. A discussion on it can be found in 3.2.5; The ideal gas limit is reproduced under $\lambda \approx \lambda_0$, for as can be seen in fig. 3, $|R'| < \infty$ is fulfilled. Then
$$R' \to R \tag{91}$$
and accordingly
$$\lambda \to (R^3 - R'^3)/R'^3 \to 0 \tag{92}$$

3.2.4 The Employed Approximation for λ

The way that approximation is introduced into this approach, is the termination of (83) at some order and then using the compatibility condition (64) as the second equation for solving for λ and R'. Depending on where (83) is terminated, the values of λ, λ_0 and λ_1 are different. For ease of computation, (83) will be terminated at 0^{th} order, so $\lambda \approx \lambda_0$ and $\lambda_1 \approx 0$. To be more transparent:

$$d(r) \approx e^{-\beta u(r)} \tag{93}$$

will be assumed. Executing the integral (58) and using the chosen approximation (93):

$$\begin{aligned}\lambda &= 3 \int_1^\infty \mathrm{d}s\, s^2\, d(sR')\, \beta u(sR') \\ &= e^{-\beta h}\, \beta h \int_1^{2R/R'} \mathrm{d}s\, \frac{\partial}{\partial s}\left[s^3\right] \\ &= e^{-\beta h}\, \beta h \left(\left(\frac{L}{R'}\right)^3 - 1 \right)\end{aligned} \tag{94}$$

which together with (64) closes the relationship between R' and λ, allowing to solve for both by inserting the compatibility condition ${R'}^3(1+\lambda) = R^3\xi$:

$$\lambda = e^{-\beta h} \cdot \beta h \cdot \left(8\frac{1+\lambda}{\xi} - 1 \right) \tag{95}$$

which can be rearranged into $\lambda = e^{-\beta h}\, \beta h \cdot 8\lambda/\xi = (1-\xi)\, \beta h\, (8/\xi - 1)$ and finally to

$$\lambda = \frac{(8-\xi) \cdot e^{-\beta h}\, \beta h}{\xi \;-\; 8\, e^{-\beta h}\, \beta h} \tag{96}$$

Even in this approximation, in the limit $\beta h \to \infty$ all the $e^{-\beta h}\beta h$ converge to 0 and all loose ξ to 1, so λ goes to $7 \cdot 0/(1 - 8 \cdot 0) = 0$. The explicit expression for (R'/R) can similarly be determined to

$$\left(\frac{R'}{R}\right)^3 = \frac{1 - e^{-\beta h}(1 + 8\beta h)}{1 - e^{-\beta h}\beta h} \tag{97}$$

which is plotted in fig. 3.

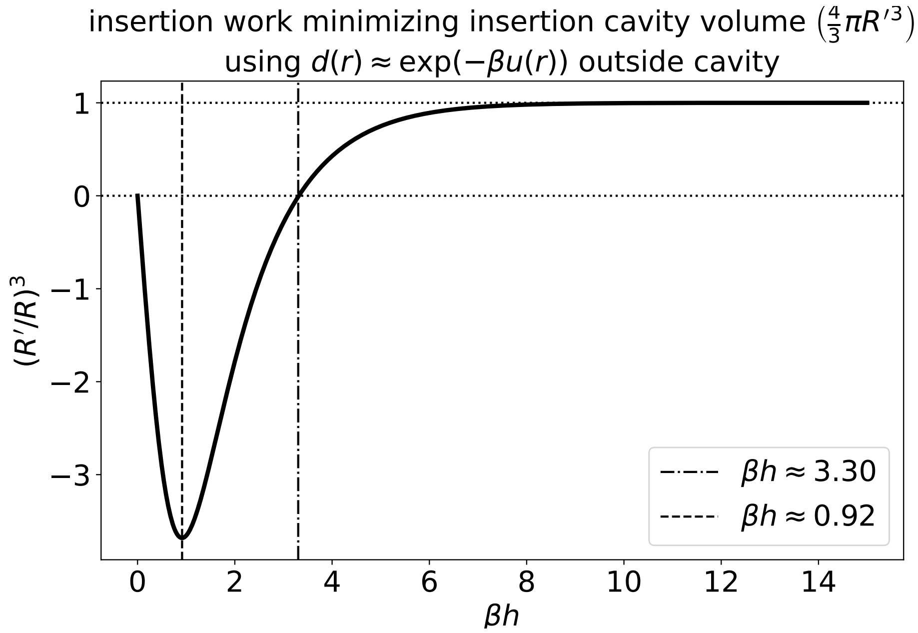

Figure 3: The fraction $(R'/R)^3$, where $\frac{4}{3}\pi R'^3$ is the volume necessary to minimize particle insertion work in the particle-insertion-work approach and $\frac{4}{3}\pi R^3$ is the particle's volume of influence (i.e. sphere with a radius of half the interaction range L), if assuming $\lambda \approx \lambda_0$ for (83). The appearance of negative R' is discussed in sec. 3.2.5.

3.2.5 Negative R'

As can be seen in fig. 3, R' can become negative under $\lambda \approx \lambda_0$. The interpretation of $\frac{4}{3}\pi R'^3$ as a volume does not make sense then. At best, one my look back to the expressions for particle insertion work (56)

$$W = p \cdot \left(\frac{4}{3}\pi R'^3\right) + W_{\text{int}} + \cdots \tag{98}$$

and notice, that if $R' < 0$, then increasing pressure decreases the reversible work of particle insertion. But this interpretation does not resolve the issue and has no other basis or motivation.

There is also the issue of R' appearing as the lower bound of integration. For in (58) a negative starting radius is nonsensical. Also, $g(r)$ and $y(r)$ are not defined for $r < 0$. Thus, when naively evaluating the integral, like in (94), the expression on the other side is technically speaking just a guess on what expression for λ will yield proper physical results. It thus appears, that there is no mending to this problem and that $R' < 0$ marks at the limits of applicability of the $\lambda \approx \lambda_0$ derived expressions.

It is plausible however, that the exact λ would resolve this issue. There are three reasons for this:

1. In fig. (12) one can observe, that (though overestimating the exact values by a lot), the φ_{PIW} structure function has the following feature, that φ_{BH} lacks: that the $\beta h = 3$ slope inside is the one growing the fastest toward $r \to 0$ (for details, see sec. 4.2). This may just be a coincidence though.

2. The assumptions and steps towards deriving φ_{PIW}, namely

   (a) Enforcing the exact low density limit expression

   (b) Adding an approximate expression for overlap energy to insertion work

   (c) Solving the equations resulting from this

   appear to be sound. If λ was computed exactly and yet the appearance of negative lengths/volumes persisted, that would be surprising.

3. $\lambda \approx \lambda_0$ lacks all number density dependence. Because λ is inserted directly into the expression for $\partial\varphi/\partial n_3$ (59), if it does not contribute in proper amounts compared to hard-sphere/entropy part (in the form of $\beta p(R'/R)^3$), then R' taking on wrong values is not as surprising anymore.

   So while full virial expansion beyond third order in density is successfully dodged for the hard sphere contribution via Fundamental Measure Theory, φ_{PIW}'s apparent sensitivity to the quality of the energy term still may yet necessitate high order data to perform.

To comment on the second point: in general, it can happen that in the virial expansion high orders of number density still contribute major features to the thermodynamics of a problem. Computing higher orders of λ becomes tedious quickly though. For example, when going up to three particle correlations, i.e. λ_1, solving for R' and λ includes a polynomial of degree six, that e.g. the `sympy.solve` function from `sympy 1.11.1` did not find an exact solution for (appearently not even having the means of finding the complex solution). That probably means that an iterative numerical solution scheme would have to be employed, if one were to include that next order in n to λ.

4 Comparing the Functionals

4.1 Overview

The following models will be compared with each other in their predictions of short range order (sec. 4.2) in the bulk fluid:

1. *Barker-Henderson Radius Hard Sphere Gas with energy term* (BH, φ_{BH}), see the definition in equation 43.
2. *Barker-Henderson Radius Hard Sphere Gas* ***without*** *energy term* (BH, Φ_{BH}), which is the excess free energy density φ_{BH} from definition in equation 43, but without the interaction term φ_{int}.
3. *Particle insertion work* (PIW, φ_{PIW}), defined in sec. 3.2.2, with the first approximation for λ introduced in sec. 3.2.4, namely termination of (83) right at order 0.

There will also be a mention on φ_{PIW} under the approximation $\lambda \approx 0$, that serves enlightening the role of R' in the behavior of φ_{PIW}. The results of that comparison will be used to rate the approaches. A comment on their low density limit (sec. 4.3) follows that discussion, which bases its claims on the short range order results. The structure function plots can be found in appendix A.

4.2 Bulk Fluid Short Range Order

Interacting fluids display short range order, described by the radial distribution function $g(r)$. This short range order determines thermodynamic quantities, like internal energy (see the energy term3.1), pressure

$$\frac{\beta p}{n} = 1 - \frac{2}{3}\pi n \int_0^\infty \mathrm{d}r\, r^3\, \frac{\partial\, \beta u(r)}{\partial r}\, g(r) \tag{99}$$

or isothermal compressibility.

$$\frac{\partial n}{\partial(\beta p)} = 1 + n \cdot \int_0^\infty 4\pi r^2\, \mathrm{d}r\, h(r) \tag{100}$$

where $h(r) = g(r) - 1$[8]. Looking at $g(r)$ quality thus goes a long way in assessing the quality of the functionals in as whole. The structure function

$h(r)$ is compared with the results from Metropolis Monte Carlo Simulations[14] and the numerical computation of Ornstein-Zernike-Closures[15].

The Monte Carlo Simulations were performed in the canonical ensemble for 6912 particles in a cubic simulation domain under periodic boundary conditions, their validity verified by comparing the results of both random and crystalline initial conditions.

An explaination of the term "Percus-Yervick-Closure" is still necessary: exactly solving the Ornstein-Zernike equation is a problem as difficult as computing the partition function exactly, as it involves knowing the radial distribution function $g(r)$ exactly. For results, an approximation has to be introduced. A Fundamental Measure Theory excess free energy density for example provides an approximate $c(r)$. A well established possibility however, is to introduce an approximate second relationship between $c(r)$ and $g(r)$. Such a relationship is then called a closure-relation. One of the most prominent for hard spheres is the Percus-Yervick-Closure

$$c(r) \approx g(r) \left(1 - e^{+\beta u(r)}\right) \tag{101}$$

Computing Bulk Fluid Radial Distribution Function To compute the bulk fluid short range order from an excess free energy density φ, in a first step the direct correlation function is computed for the bulk fluid according to (30), resulting in

$$c(|\boldsymbol{r} - \boldsymbol{q}|) = -\sum_{\alpha} \sum_{\beta} \frac{\partial^2 \varphi}{\partial n_\alpha \partial n_\beta} \, \omega_\alpha \otimes \omega_\beta(\boldsymbol{r} - \boldsymbol{q}) \tag{102}$$

Computing all appearing second derivatives and cross correlations (the latter are listed in Appendix D) and setting the vectorial densities to 0 as well es the scalar densities to (19) then renders a direct correlation function $c(r)$. Now $c(r)$ can be inserted into the Ornstein-Zernike-equation (29) and solved for h. Solving (29) in Fourier-Space renders in principle gives an exact solution via inverse Fourier-Transoform, but long range oscillations in the spectrum due to the discontinuities in the problem led to various difficulties. So instead $c(r)$ is inserted into the fixed point iteration scheme (123) described in Appendix C.

---

[14] Monte Carlo simulation data were provided by courtesy of Robert F. B. Weigel

[15] Percus-Yervick closure to the Ornstein-Zernike equation was provided by courtesy of Matthias Gimperlein

Note that the fixed point iteration produces kinks in its $h(r)$ towards $r = 0$. They vanish at high iteration counts. They vanish at such a slow pace however, that doing so was not worth it, especially given that they are very small.

$h(r)$-sloping within $r < L$ As can be seen in any of the figures in appendix A, the data points of the Monte Carlo simulation display falling slopes with in the interaction distance range $r < L$. It is important to keep in mind, that $g(r)$ is a radial profile, meaning not $g(r)\,\mathrm{d}r$, but $g(r)\,4\pi r^2\,\mathrm{d}r$ is proportional to the number of particles found in the interaction distance shell $[r, r + \mathrm{d}r]$. If the probability density ρ of finding a particle at any of the distances $r < L$ was equal for all of them, that would force $n \cdot g(r) = \rho/(4\pi r^2)$. Any deviation of $g(r)$ from an inverse square relationship within interaction distance should thus be considered interesting.

4.2.1 Barker-Henderson Radius Hard Sphere Gas plus Energy Term Approach

In fig. 9 φ_{BH} can be seen to match up rather well with Monte Carlo Simulations. It does however not feature the very steep slope of $\beta h = 3$.

An interestingly close match up is observed with the Percus-Yervick-Closure in fig. 10. For all depicted interaction distances r and stepsizes βh the two plots almost align. To investigate this one a little bit further: φ_{BH} fulfills the Percus-Yervick closure relation (101) much better than φ_{PIW} does, as is depicted in 4.

Role of the Energy Term φ_{int} of φ_{BH} Leaving out the energy term φ_{int} from equation 43 results in the bulk fluid structure shown in fig. 11 (which is also depicted with the label Φ_{BH} in fig. 5, 6, 7, 8)

- Significant differences between the $h(r)$ produced by the functional with energy and the $h(r)$ of the one without energy term are seen for all βh within $r < L$. For $\eta = 0.3$ the slope growing towards $r \to 0$ of the Monte-Carlo-Data is absent in the $h(r)$ produced by Φ_{BH}, but is qualitatively reproduced in $\varphi_{\mathrm{int}} + \Phi_{\mathrm{BH}}$.

  Looking at $\eta = 0.3$: at stepsize $\beta h = 1$ the φ_{BH} prediction fits particularly well and the Φ_{BH} prediction particularly poorly, the latter not even producing an inverse square decaying $h(r)$ within $r < L$. The

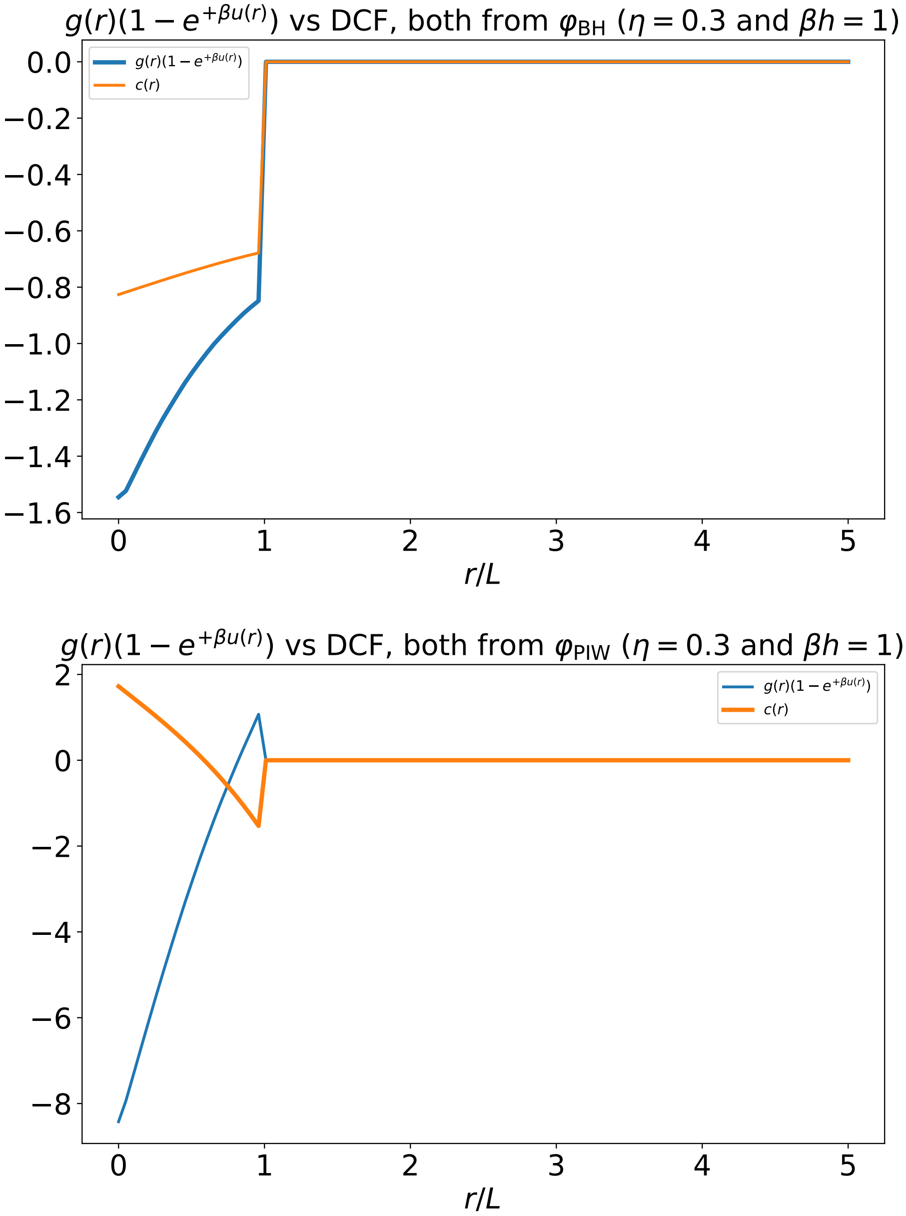

Figure 4: Comparing how much φ_{BH} (the upper plot) and φ_{PIW} (the lower plot) fulfill (101), by plotting both $c(r)$ and $g(r)(1-e^{+\beta u(r)})$ at packing fraction $\eta = 0.3$ and stepsize $\beta h = 1$.

conclusion is, that the zenith of the energy term's importance in φ_{BH} is found at step sizes around $\beta h = 1$, as would be expected from (42). This observation also goes to show, that the slopes at $r < L$ are only accounted for in the energy term. So for particle separations r within interaction distance L, φ_{int} is central to giving meaningful results.

- For large βh (in fig.s 9 and 11 that is $\beta h = 6, 10$) the region $r > L$ works equally well with and without energy term, as should be expected: the analytical $\beta h \to \infty$ limit of φ_{BH} is White Bear II, because energy contributions loose their significance.

- As would be expected of the lower stepsizes (like $\beta h = 1$), adding the energy term indeed improves the functional's $h(r)$ quality at $\beta h = 1$. However, the reproduction of the $\beta h = 3$ structure function outside $r > L$ is improved without the energy term (11) compared to with it (9). So the energy term's influence at $\beta h = 3$ is too large compared to what is seen in simulation.

4.2.2 Particle Insertion Work Approach

In fig. 12 φ_{PIW} under $\lambda \approx \lambda_0$ (in reference to equation 83) has the wrong qualitative behavior at $\beta h \leq 3$. First of all, $h(r)$ starts taking on impossible values below -1. Besides that, at the distance $r = L$, $h(r)$ should be decaying, not rising. It is probably not a coincidence, that $\beta h = 1, 3$ are within the βh-range that R' is negative in (see fig. 3) and goes to show the invalidity of results in $\{\beta h \mid R' < 0\}$. The $\beta h = 6, 10$ results are sound though. A discussion of negative R' can be found in section 3.2.5.

However, φ_{PIW} (fig. 12) shares a feature with the Monte Carlo data, that φ_{BH} (fig. 9) does not, namely that in the region $r < L$ the $\beta h = 3$ curve slopes towards $r = 0$ the fastest. The feature persists, if one uses the approximation $\lambda \approx 0$ instead (see fig. 13), meaning it is not a consequence of R' taking on negative values.

Note that in fig. 13, no impossible $h(r)$ values occur and the inward sloping at $r < L$ still happens, further demonstrating that the impossible h-values in fig. 12 are the consequence of negative R'. That any sloping still occurs is interesting, because as is established in the sec. 4.2.1 on the role of φ_{int}, in φ_{BH} all of the $r < L$ sloping of the structure function is caused by the energy term.

4.2.3 Direct Comparisons

In fig. 6,7,8 the structure functions predicted by φ_{PIW}, φ_{BH} and Φ_{BH} are compared directly with each other at $\eta = 0.3$.

- For the stepsize $\beta h = 6$, where the oddities in the behavior of the $\lambda \approx \lambda_0$ approximation to φ_{PIW} do not dominate the prediction anymore, no solid indication of the sloping observed in the Monte Carlo Data are seen for φ_{BH} or Φ_{BH} or under Percus-Yervick closure. It is qualitatively seen for φ_{PIW} however, both sloping and curvature go in the correct direction.
- For $\beta h = 6$ the structure functions φ_{BH} and Φ_{BH} overlap, because $R_{\mathrm{BH}}/R = \xi$ (35) is ≈ 1 as seen in fig. 1. Same goes for $\beta h = 10$, where φ_{PIW} also joins in, such that all predicted $h(r)$ overlap in their common hard sphere limit.

4.3 Low Density Limit Expression

By construction (50), the low density limit of φ_{PIW} is

$$\int \varphi_{\mathrm{PIW}} \overset{n\to 0}{\approx} \int \xi(n_0 n_3 + n_1 n_2 - \boldsymbol{n}_1 \boldsymbol{n}_2) = -\frac{1}{2}\int_1\int_2 f_{12} n_1 n_2 \tag{103}$$

which acknowledges the formal functional expansion of βF_{ex} [12]

$$-\beta F_{\mathrm{ex}} = \frac{1}{2}\int_1\int_2 f_{12} n_1 n_2 + \frac{1}{6}\int_1\int_2\int_3 f_{12} f_{23} f_{31}\, n_1 n_2 n_3 \quad + \quad \mathcal{O}(n^4) \tag{104}$$

based on cluster expansion.

The limit (104) is not reproduced in the Barker-Henderson-based functional φ_{BH}. The energy term is already quadratic in the $\{n_\alpha\}$, so it is in low density form already. The chain rule shows, that the low density limit of the hard sphere contribution $\int \Phi_{\mathrm{BH}}$ consists of replacing the $\{n_\alpha\}$ with their appropriately Barker-Henderson-rescaled counterparts (36), such that

$$\int \varphi_{\mathrm{BH}} \overset{n\to 0}{\approx} \int e^{-\beta h}\beta h(n_0 n_3 + n_1 n_2 - \boldsymbol{n}_1 \boldsymbol{n}_2) + \int \xi^3(n_0 n_3 + n_1 n_2 - \boldsymbol{n}_1 \boldsymbol{n}_2) \tag{105}$$

This is dot damning however. Virial expansion often converges slowly, i.e. the higher orders are siginificant even when compared to low orders (or phrased yet another way: n-particle interactions are not negligible). The results for the fluid structure (see fig. 9) successfully reproduce the Percus-Yervick-Closure results. That suggests, that refining φ_{BH} could be worthwhile. So rather than criticizing φ_{BH} for failing to reproduce the low density limit of (104), the necessity of analytically enforcing that limit should be called into question in the case of the step-potential, if the aim is trying to extract information about bulk fluid structure.

5 Summary and Conclusion

In this bachelor's thesis, two approximations to step potential excess free energy have been derived, that are formulated with concepts introduced by Fundamental Measure Theory. By reweighting the weighted densities of the White Bear II excess free energy density in a manner inspired by the Barker-Henderson hard sphere diameter and adding an energy term, a result close to the Percus-Yervick closure to the Ornstein-Zernike equations has been achieved. An approach that attempts to emulate the way Rosenfeld derived his original Fundamental Measure Theory [10] has also been discussed. It under the line performs worse than the Barker-Henderson + energy term approach when approximations of similar quality are inputted, because the effective hard sphere radius R' it introduces is more deeply linked with the energy expression (64). Yet, expansion (83) provides a recipe to improve upon these approximations. But a further, numerical investigation of higher orders of (83) may conclude, that accuracy improves too slowly to justify the effort. However, the accuracy of the energy contribution to φ_{BH} is (in the current form of the approach) at its limit, as explained at the end of sec. 3.1.1. What further numerical investigation can be done, is thus more obvious for φ_{PIW}.

A Plots of Structure Functions and Illustrative Figures From the Discussion

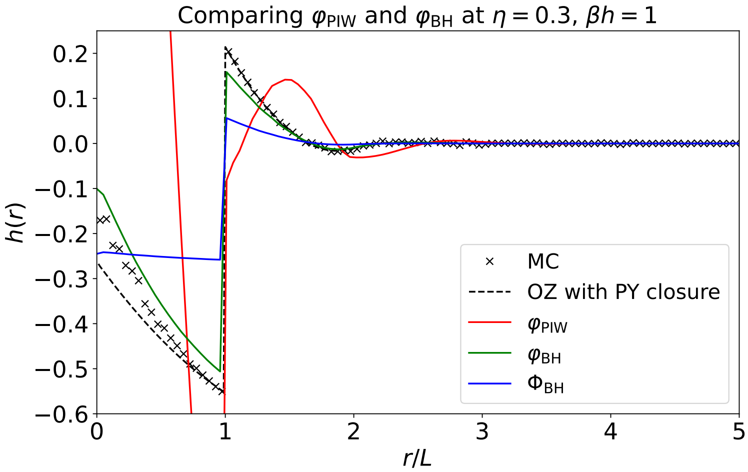

Figure 5: Comparing the result of $h(r)$ from the particle-insertion-work approach (denoted φ_{PIW}) with the $h(r)$ from the Barker-Henderson- White Bear II approach **with** energy term (denoted φ_{BH}) and also a version **without** energy term (denoted Φ_{BH})

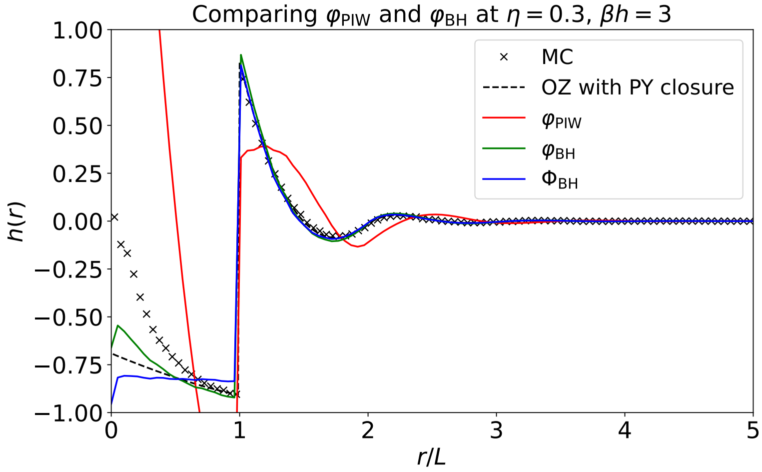

Figure 6: Comparing the result of $h(r)$ from the particle-insertion-work approach (denoted φ_{PIW}) with the $h(r)$ from the Barker-Henderson- White Bear II approach **with** energy term (denoted φ_{BH}) and also a version **without** energy term (denoted Φ_{BH})

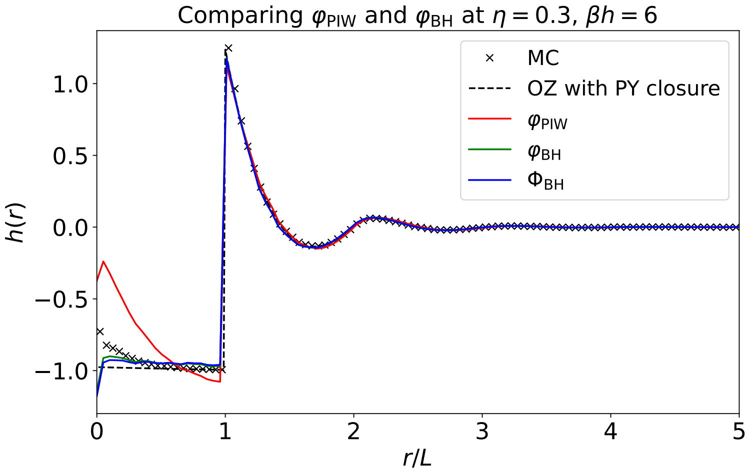

Figure 7: Comparing the result of $h(r)$ from the particle-insertion-work approach (denoted φ_{PIW}) with the $h(r)$ from the Barker-Henderson- White Bear II approach **with** energy term (denoted φ_{BH}) and also a version **without** energy term (denoted Φ_{BH})

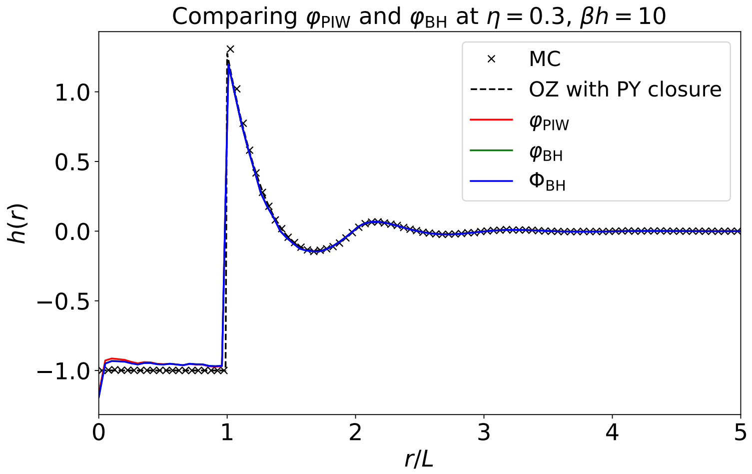

Figure 8: Comparing the result of $h(r)$ from the particle-insertion-work approach (denoted φ_{PIW}) with the $h(r)$ from the Barker-Henderson- White Bear II approach **with** energy term (denoted φ_{BH}) and also a version **without** energy term (denoted Φ_{BH})

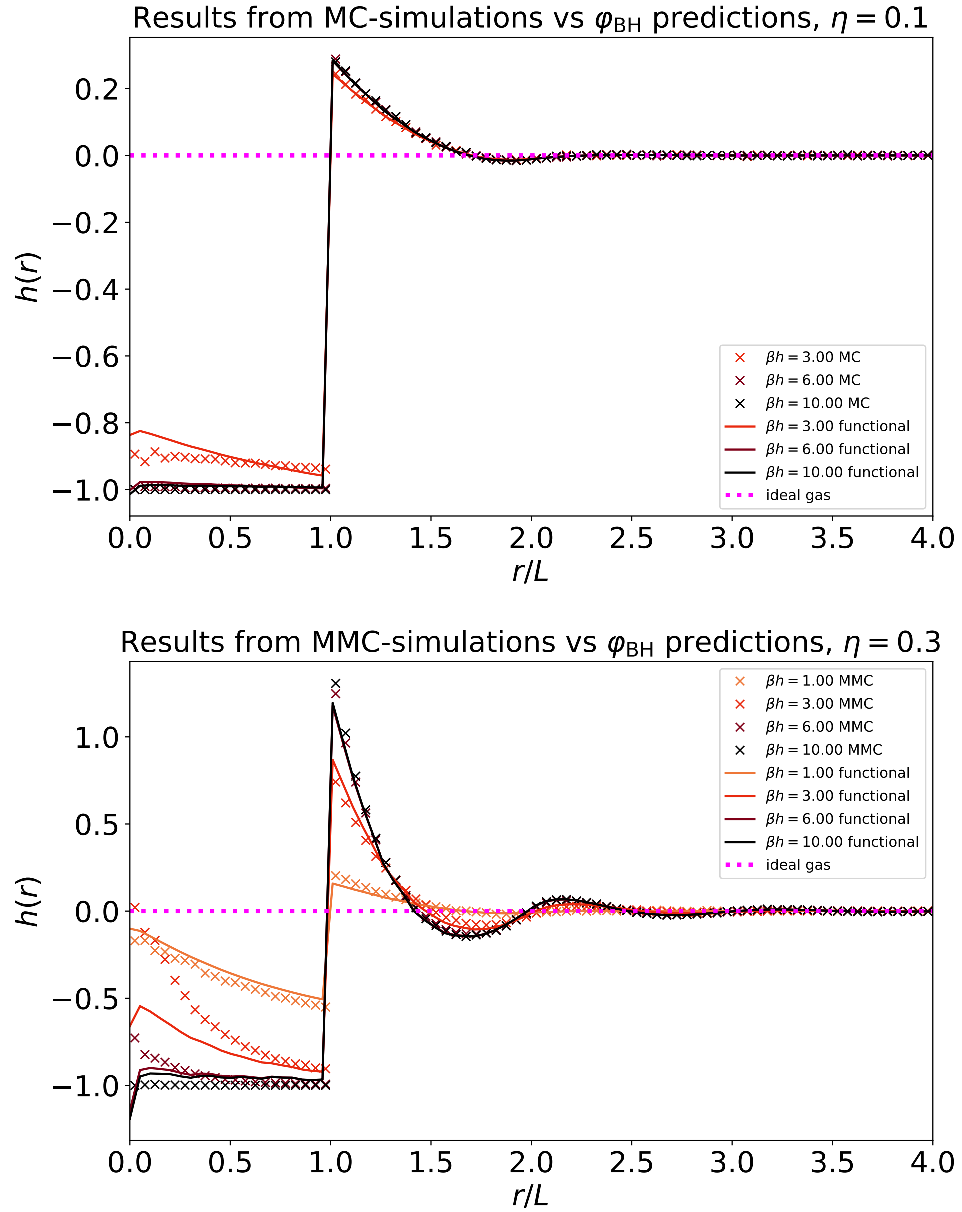

Figure 9: Comparing the result of $h(r)$ for the Barker-Henderson- White Bear II **including** the energy term from (42) Fundamental Measure Theory functional φ_{BH} against Monte Carlo Simulations. The match up is satisfactory.

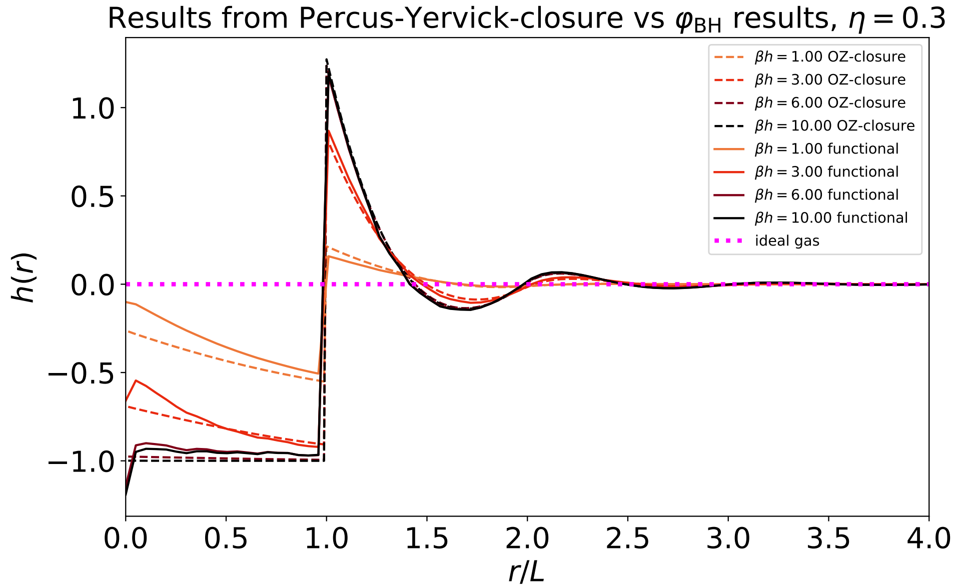

Figure 10: Comparing the result of $h(r)$ for the Particle Insertion Work Fundamental Measure Theory functional φ_{BH} against the result from Percus-Yervick closure to the Ornstein-Zernike equation. The match-up is very close.

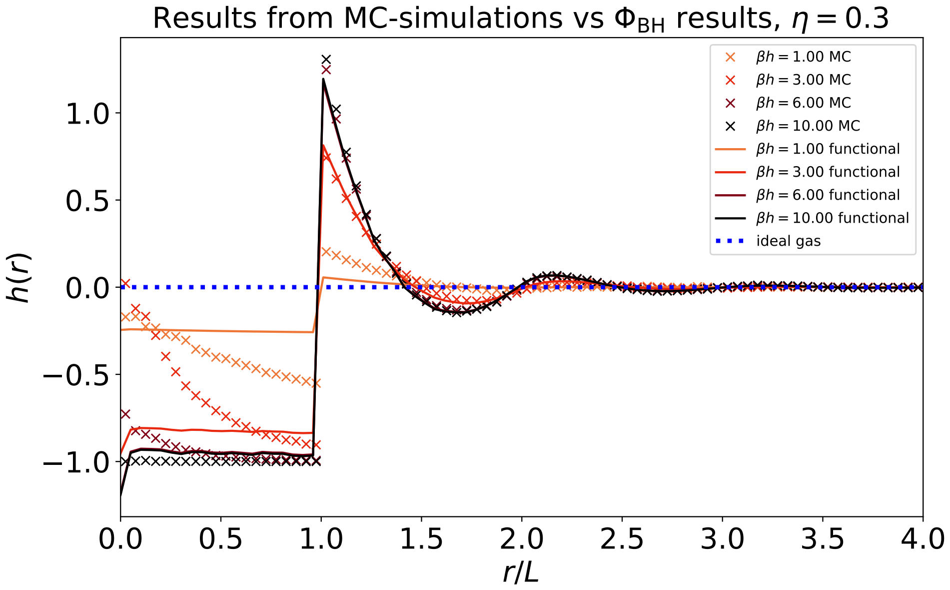

Figure 11: Comparing the result of $h(r)$ for the Barker-Henderson- White Bear II **not including** the energy term from (42) Fundamental Measure Theory functional, Φ_{BH}, against Monte Carlo Simulations. The differences to 9 demonstrate some of the influence of the energy term.

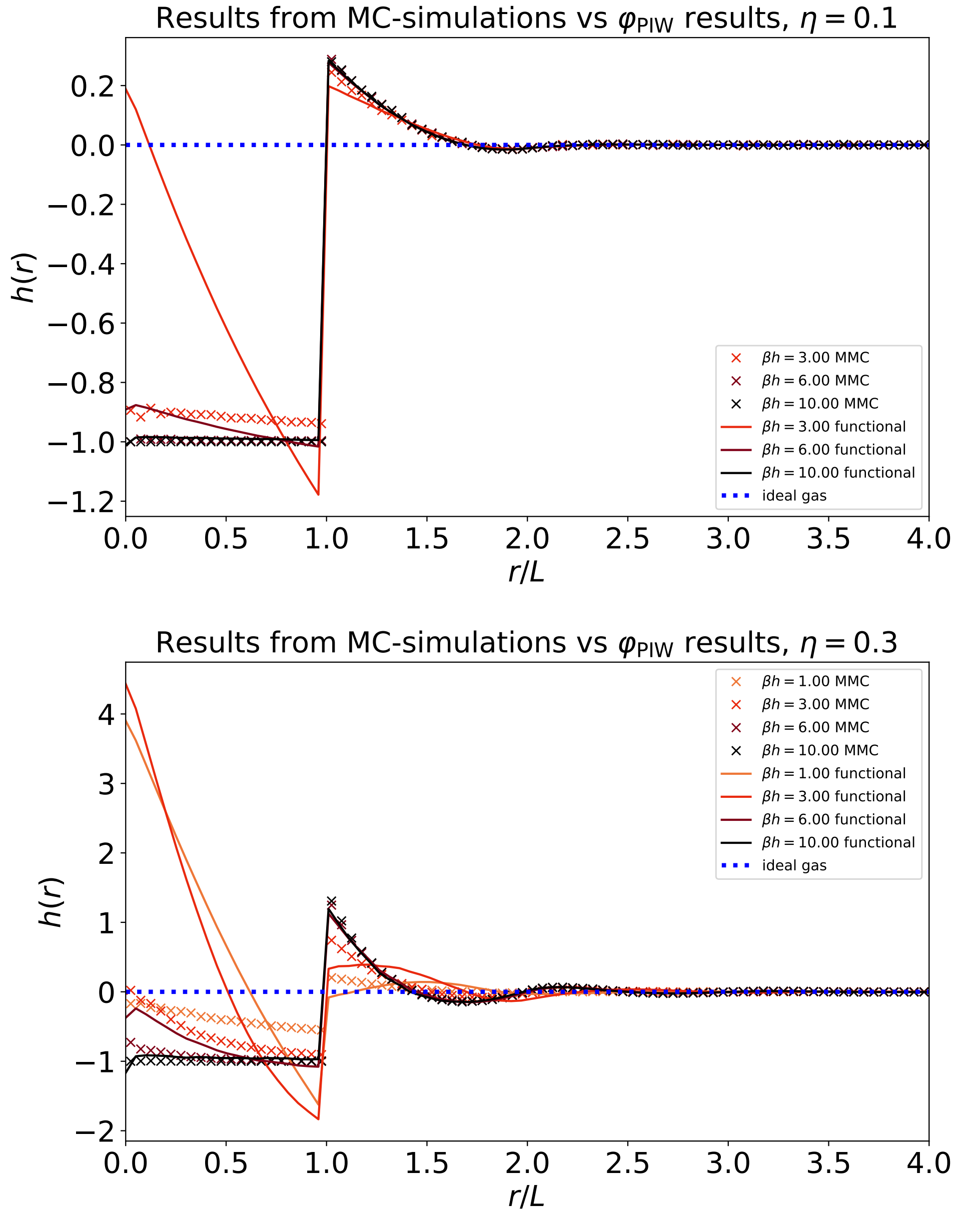

Figure 12: Comparing the result of $h(r)$ for the Particle Insertion Work Fundamental Measure Theory functional φ_{PIW} against Monte Carlo Simulations. The approximation used to compute the $h(r)$ in both images was $\lambda \approx \lambda_0$. Though physically sound for $\beta h > 3$, the results are bad in the region where $R' < 0$, which is probably not a coincidence.

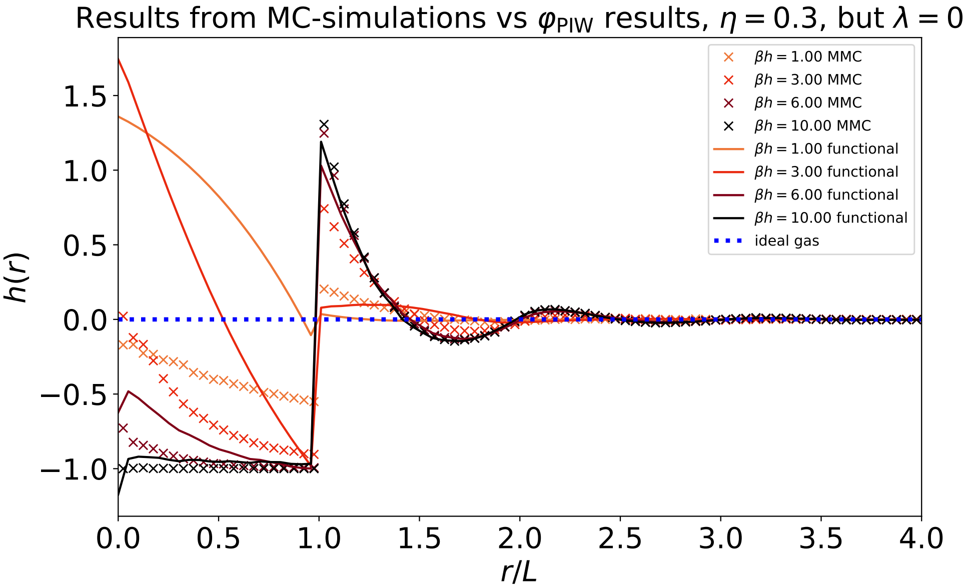

Figure 13: Comparing the result of $h(r)$ for the Particle Insertion Work Fundamental Measure Theory functional φ_{PIW} against Monte Carlo Simulations. However in contrast to 12 $\lambda \approx 0$ is used as λ-approximation.

B Appendix Delegated Computation

Determining the Integration Constants $f_4(0)$ and $f_5(0)$ from the φ_{PIW} Derivation

Relating $f_4(0)$ and $f_5(0)$ The integration constants $f_4(0)$ and $f_5(0)$ coming up in sec. 3.2.1 are related by the system's direct correlation function. In the bulk fluid all of the second φ-derivatives from

$$\frac{\delta^2 \beta F_{\mathrm{ex}}}{\delta n(\boldsymbol{q})\, \delta n(\boldsymbol{r})} = \sum_\alpha \sum_\beta \int \mathrm{d}^3 x \frac{\partial^2 \varphi}{\partial n_\beta \partial n_\alpha}(\boldsymbol{x})\, \omega_\beta(\boldsymbol{x}-\boldsymbol{q})\, \omega_\alpha(\boldsymbol{x}-\boldsymbol{r}) \tag{106}$$

are not explicitly position-dependent. The transformation $\boldsymbol{x} \mapsto \boldsymbol{x}+\boldsymbol{r}$ turns the remaining integral into the cross correlation $\omega_\alpha \otimes \omega_\beta(\boldsymbol{r}-\boldsymbol{q})$, allowing a more condensed rephrasing of the second variational derivative expression. By equation (12) one gets the relationship

$$-\, c(|\boldsymbol{r}-\boldsymbol{q}|) = \frac{\delta^2 \beta F_{\mathrm{ex}}}{\delta n(\boldsymbol{q})\, \delta n(\boldsymbol{r})} = \sum_\alpha \sum_\beta \frac{\partial^2 \varphi}{\partial n_\alpha \partial n_\beta}\, \omega_\alpha \otimes \omega_\beta(\boldsymbol{r}-\boldsymbol{q}) \tag{107}$$

The cross correlations whose coefficients in c contain f_4 or f_5 turn out to be $\omega_2 \otimes \omega_2$ and $\boldsymbol{\omega_2} \otimes \boldsymbol{\omega}_2$[16]. Both of these diverge for $r \to 0$, which means they have to be handled carefully. They are among other things related by

$$\lim_{r\to 0} \frac{\boldsymbol{\omega}_2 \otimes \boldsymbol{\omega}_2(r)}{\omega_2 \otimes \omega_2(r)} = 1 \tag{108}$$

as is shown by the explicit expressions for $\omega_\alpha \otimes \omega_\beta$ computed in the appendix (sec. D). Writing out their contribution to $c(r)$ in is a matter of computing the according second derivatives of φ. The result of that is

$$\begin{aligned} c(r) &= \cdots + (3 \cdot 2 \cdot n_2\, f_4\, \omega_2 \otimes \omega_2(r) + 2 \cdot 1 \cdot n_2\, f_5\, \boldsymbol{\omega}_2 \otimes \boldsymbol{\omega}_2(r)) \\ &= \cdots + 2n_2 \left(3\, f_4 + f_5 \frac{\boldsymbol{\omega}_2 \otimes \boldsymbol{\omega}_2(r)}{\omega_2 \otimes \omega_2(r)} \right) \omega_2 \otimes \omega_2(r) \end{aligned} \tag{109}$$

---

[16] Note that in (106) the $\boldsymbol{\omega}_2$ are actually not contracted with each other, but instead with the gradients $\partial/\partial \boldsymbol{n}_2$ of φ. But in the present functional $\boldsymbol{n}_2$ appears only in the form $\boldsymbol{n}_2 \mathbb{I} \boldsymbol{n}_2$, meaning the hessian $\partial^2\varphi/\partial \boldsymbol{n_2} \partial \boldsymbol{n}_2$ is a function proportional to the unit matrix $\mathbb{I}$; contracting two vectors with $\mathbb{I}$ is, of course, the same as the standard dot product.

dividing both sides by $\omega_2 \otimes \omega_2(r) = \pi R \, [r/L]^{-1} \, \Theta(L-r)$ (while considering only interaction distances $r < L$) results in

$$\frac{1}{\pi R} \frac{r}{L} \, c(r) = \cdots + 2n_2 \left(3 \, f_4 + f_5 \frac{\boldsymbol{\omega}_2 \otimes \boldsymbol{\omega}_2(r)}{\omega_2 \otimes \omega_2(r)} \right) \tag{110}$$

This division not only mends the $\omega_2 \otimes \omega_2(r)$-divergence, but because $\omega_0 \propto \omega_1 \propto \omega_2$ all terms divergent at $r \to 0$, namely the ones containing an $\omega_\alpha \otimes \omega_\beta$-factor with $\alpha, \beta \in \{0, 1, 2\}$, are have a finite limit. This permits the limit $r \to 0$, resulting in

$$0 = \cdots + 2n_2 \left(3 \, f_4 + f_5 \right) \tag{111}$$

That relationship has to hold for all densities, forcing $f_5 = -3f_4$, and in particular the sought integration constants to

$$f_5(0) = -3f_4(0) \tag{112}$$

This derivation of the $f_4(0)$-$f_5(0)$-relationship did not include any explicit expressions for f_4 or f_5. It thus holds for any (three dimensional) expression for the free energy density of the step potential, that uses Rosenfeld's ansatz while trying to be consistent with the second-order-in-density limit.

Finding the $f_4(0)$-value $f_4(0)$ is given, by enforcing that the third virial coefficient B_3^{s} is reproduced by φ's pressure equation. B_3^{s} of the step potential is proportional to B_3^{h} of the hard sphere gas, as can be seen from $f_{ij}^{\mathrm{s}} = \xi \, f_{ij}^{\mathrm{h}}$ and its formula [8]

$$\begin{aligned} -3V \cdot B_3^{\mathrm{s}} &= \int_1 \int_2 \int_3 f_{12}^{\mathrm{s}} f_{23}^{\mathrm{s}} f_{31}^{\mathrm{s}} \\ &= \xi^3 \int_1 \int_2 \int_3 f_{12}^{\mathrm{h}} f_{23}^{\mathrm{h}} f_{31}^{\mathrm{h}} \\ &= \xi^3 \cdot \left(-3V \cdot B_3^{\mathrm{h}} \right) \end{aligned} \tag{113}$$

where the hard sphere third virial coefficient is in turn given by [3]

$$B_3^{\mathrm{h}} = 10 \cdot \left(\frac{4}{3} \pi R^3 \right)^2 \tag{114}$$

It was imposed earlier, that the uniform fluid fulfills $\beta p = \partial \varphi / \partial \tilde{n}_3 + n_0 \lambda$, the third order in $n_0, \ldots, \boldsymbol{n}_2, \tilde{n}_3$ of which reads

$$\beta p = \cdots + (1 + \lambda(0)) \cdot n_0 \tilde{n}_3 \tilde{n}_3 + \frac{\partial \lambda}{\partial n_0}(0) \cdot n_0 n_0 \tilde{n}_3 + 2 \cdot n_1 n_2 \tilde{n}_3 + 2 f_4(0) \cdot n_2 n_2 n_2 + \cdots \tag{115}$$

where the vectorial weighted densities vanish because the homogeneous fluid is considered. To get the third order in n, it must be remembered, that $\tilde{n}_3$ does not depend on n linearly like the other bulk fluid weighted densities, but instead depends on it through 64 as $\tilde{n}_3 = (\xi/(1+\lambda(n))) \cdot \left(\frac{4}{3}\pi R^3\right) \cdot n$. $\tilde{n}_3$ is, to first non-vanishing order, linear in n, so that the lowest order expansion in n, namely

$$\frac{\xi}{1+\lambda(0)} \cdot \left(\frac{4}{3}\pi R^3\right) \cdot n \tag{116}$$

has to be inserted for $\tilde{n}_3$

$$\begin{aligned} \beta p = \dots &+ \frac{\xi}{1+\lambda(0)} \left(\xi \cdot n_0 n_3 n_3 + \frac{\partial \lambda}{\partial n}(0) \cdot n_0 n_0 n_3 + 2 \cdot n_1 n_2 n_3\right) \\ &+ 2 f_4(0) \cdot n_2 n_2 n_2 \\ &+ \cdots \end{aligned} \tag{117}$$

In reference to the expansion of λ found in (83)

$$\begin{aligned} \lambda_0 &:= \lambda(0) \\ \lambda_1 &:= \frac{\partial \lambda}{\partial n}(0) \end{aligned} \tag{118}$$

are defined. Now the virial expansion

$$\beta p = \dots + B_3^{\mathrm{s}} \cdot n^3 + \cdots \tag{119}$$

can be inserted into βp, focusing on the third order in number density. If M_α is the sphere's fundamental measure α, e.g. $M_2 = 4\pi R^2$, then comparison of the n^3 coefficient on both sides of (117) results in the equation

$$\xi^3 \cdot 10 \cdot {M_3}^2 = 2\, f_4(0) M_2 M_2 M_2 + \frac{\xi}{1+\lambda_0} \left(\xi\, {M_3}^2 + \lambda_1\, M_3 + 2\, M_1 M_2 M_3\right) \tag{120}$$

where (113) was inserted. Solving for $f_4(0)$

$$\begin{aligned} f_4(0) &= \frac{1}{2}\left(10\xi^3 \frac{{M_3}^2}{{M_2}^2} - \frac{\xi}{1+\lambda_0}\left(\xi \frac{{M_3}^2}{{M_2}^3} + \lambda_1 \frac{M_3}{{M_2}^3} + 2\frac{M_1 M_2 M_3}{{M_2}^3}\right)\right) \\ &= \frac{1}{2}\left(10\xi^3 \frac{1}{36\pi} - \frac{\xi}{1+\lambda_0}\left(\xi \frac{1}{36\pi} + \lambda_1 \frac{1}{12\pi}\frac{1}{R^3} + 2\frac{1}{12\pi}\right)\right) \\ &= \frac{1}{2}\frac{1}{36\pi}\left(10\xi^3 - \frac{\xi}{1+\lambda_0}\left(\xi + \lambda_1 \frac{36\pi}{12\pi}\frac{1}{R^3} + 2\frac{36\pi}{12\pi}\right)\right) \\ &= \frac{1}{24\pi} \cdot \frac{1}{3}\left(10\xi^3 - \frac{\xi}{1+\lambda_0}\left(\xi + \frac{3 \cdot \lambda_1}{R^3} + 6\right)\right) \end{aligned} \tag{121}$$

In the limit $\beta h \to \infty$, ξ becomes 1. Recall that λ has to be approximated by terminating (83) at some point. If $\lambda_0, \lambda_1 \to 0$ (like in the approximation $\lambda \approx \lambda_0$ does), (121) reproduces the hard sphere value

$$f_4^{\mathrm{h}}(0) = 1/24\pi \tag{122}$$

For the ideal gas $\beta h \to 0$, $f_4(0)$ approaches 0, because all the ξ do.

C Computing $g(r)$ from $c(r)$

Fixed Point Iteration on Ornstein-Zernike Equation

One can used fixed point iteration (an example of which is in [12] on Picard Iteration on density profiles) to find for a given $c(r)$ the $h(r)$ fulfilling the Ornstein-Zernike-equation $h = c + n \cdot c * h$, namely the sequence $\{h_j\}$ given by

$$h_{j+1} = c + n \cdot c * h_j \tag{123}$$

In the practice of working with the considered functionals, this scheme diverged close to the hard sphere limit at packing fractions beyond about $\eta = 0.1$ though. A way to get around this, is to introduce a mixing parameter $0 < q < 1$ (also found in [12]).

$$h_{j+1} = q \cdot (c + n \cdot c * h_j) + (1 - q) \cdot h_j \tag{124}$$

which for $q < 0$ has convergence for a broader selection of direct correlation functions. A useful way to think about q, is that scheme (124) decreases the influence of $n \cdot c * h_j$ relative to (123) in determining the next member of the sequence. Low q have the disadvantage of including barely any information from the convolution. Concretely, this means convergence then becomes very slow even in principle; in practice, where some sort of approximate representation by an array has to happen, additionally the accuracy of the result suffers.

D Explicit Expressions

Explicit Expressions for The Weight Function Cross-Correlations When computing the weight function cross correlations, integrals of the following four types appear:

1. *sphere-sphere overlap.* This one is found when computing $\omega_3 \otimes \omega_3(r)$ and per geometric arguments works out to

$$\int \mathrm{d}^3 q\, \Theta(R - |\boldsymbol{q}|)\, \Theta(R - |\boldsymbol{q} + \boldsymbol{r}|) = \frac{4}{3}\pi R^3 \cdot \left(1 - \frac{3}{2}\left[\frac{r}{L}\right] + \frac{1}{2}\left[\frac{r}{L}\right]^3\right) \cdot \Theta(L - r)$$

   where $L := 2R$.

2. *sphere-shell overlap.* All versions of this case appear in the expression for $c_{\mathrm{RF}}(r)$. The integral to be computed is

$$\int \mathrm{d}^3 q\, \delta(R - |\boldsymbol{q}|)\, \Theta(R - |\boldsymbol{q} + \boldsymbol{r}|)$$

   picking spherical coordinates, such that $\boldsymbol{r}$ lies on the z-axis and that the latitudinal angle ϑ lines up exactly with the angle between $\boldsymbol{r}$ and $\boldsymbol{q}$, the integral can be rewritten as

$$\int_0^\infty \mathrm{d}q \int_0^\pi q\, \mathrm{d}\vartheta \int_0^{2\pi} q\, \sin\vartheta\, \mathrm{d}\varphi\, \delta(R - q)\, \Theta(R - \sqrt{q^2 + r^2 + 2qr\, \cos\vartheta})$$

   this allows integrating out q (and while at it, also φ), resulting in $q \equiv R$

$$2\pi R^2 \int_0^\pi \mathrm{d}\vartheta\, \sin\vartheta\, \Theta(R - \sqrt{R^2 + r^2 + 2Rr\, \cos\vartheta})$$

   considering $-\cos\vartheta$ the new integration variable gets rid of the $\sin\vartheta$-factor. Finding the bounds of integration imposed by $\Theta(R - \sqrt{R^2 + r^2 + 2Rr\, \cos\vartheta})$ is a matter of finding out when the argument is larger than 0, which happens for $-\cos\vartheta > r/L > 0$, where $L := 2R$

$$\begin{aligned}\int \mathrm{d}^3 q\, \delta(R - |\boldsymbol{q}|)\, \Theta(R - |\boldsymbol{q} + \boldsymbol{r}|) &= 2\pi R^2 \int_{r/L}^1 \mathrm{d}(-\cos\vartheta) \\ &= 2\pi R^2 \cdot \left(1 - \frac{r}{L}\right)\, \Theta(L - r)\end{aligned}$$

3. *shell-shell overlap.* Care has to be taken with the Dirac-δ, as

$$\delta(y(x)) = \sum_j \frac{\delta(x - x_j)}{|\partial y / \partial x(x_j)|}$$

where the x_j are the roots of y. For the integral in question reads

$$\int \mathrm{d}^3 q\, \delta(R - |\boldsymbol{q}|)\, \delta(R - |\boldsymbol{q} + \boldsymbol{r}|)$$

Switching to spherical coordinates, such that $\boldsymbol{r}$ lies on the z-axis and that the latitudinal angle ϑ lines up exactly with the angle between $\boldsymbol{r}$ and $\boldsymbol{q}$, the integral can be rewritten as

$$\int_0^\infty \mathrm{d}q \int_0^\pi q\, \mathrm{d}\vartheta \int_0^{2\pi} q\, \sin\vartheta\, \mathrm{d}\varphi\, \delta(R - q)\, \delta(R - \sqrt{q^2 + r^2 + 2qr\, \cos\vartheta})$$

which allows for integrating out q and φ. One can get rid of the $\sin\vartheta$ factor by treating $-\cos\vartheta$ as the new integration variable

$$2\pi R^2 \int_{-1}^{1} \mathrm{d}(-\cos\vartheta)\, \delta(R - \sqrt{R^2 + r^2 + 2Rr\, \cos\vartheta})$$

the derivative of the Dirac-δ's argument with respect to $-\cos\vartheta$ is

$$\frac{rR}{\sqrt{R^2 + r^2 + 2Rr\, \cos\vartheta}}$$

Evaluating that at the root of $R - \sqrt{R^2 + r^2 + 2Rr\, \cos\vartheta}$ obviously makes the denominator take on the value R. Looking at the geometry reveals $-\cos\vartheta = r/L$, where $L = 2R$, meaning

$$\delta(R - \sqrt{R^2 + r^2 + 2Rr\, \cos\vartheta}) = \frac{\delta(-\cos\vartheta - r/L)}{r}$$

To summarize

$$\int \mathrm{d}^3 q\, \delta(R - |\boldsymbol{q}|)\, \delta(R - |\boldsymbol{q} + \boldsymbol{r}|) = 2\pi R^2 \cdot \frac{1}{r} \cdot \Theta(L - r) = \pi R \left[\frac{r}{L}\right]^{-1} \Theta(L - r)$$

4. *shell-shell overlap with surface normals contraction.* Terms like $\boldsymbol{\omega}_2 \otimes \boldsymbol{\omega}_1$ include the dot product of the surface normals of the two spheres as a factor in the integrand. The cylindrical symmetry of the two intersecting spheres forces that dot product $(\boldsymbol{q}/|\boldsymbol{q}|) \cdot ((\boldsymbol{q} + \boldsymbol{r})/|\boldsymbol{q} + \boldsymbol{r}|)$ to be constant, and the mirror symmetry (because the two spheres are identical) makes the dot product's value be

$$\cos(2\alpha) = 1 - 2\sin^2\alpha$$

where 2α is the angle between the surface normals of the intersecting spheres at any given intersection point. By comparing opposite angles in the intersection of the lines indicated by the two surface normals,

$$\sin\alpha = \frac{r}{L}$$

can be deduced, L being $2R$. Besides the dot product, the integrand is the same as for the corresponding scalar weight functions. This finally shows, that

$$\int \mathrm{d}^3q\, \frac{\boldsymbol{q}}{|\boldsymbol{q}|}\cdot\frac{\boldsymbol{q}+\boldsymbol{r}}{|\boldsymbol{q}+\boldsymbol{r}|}\,\delta(R-|\boldsymbol{q}|)\,\delta(R-|\boldsymbol{q}+\boldsymbol{r}|) = \left(1-2\left[\frac{r}{L}\right]^2\right)\pi R\left[\frac{r}{L}\right]^{-1}\Theta(L-r)$$

In principle the following two integrals are also possible, though in the practice of computing the presented results, they were never necessary:

1. When the weights is are among $\alpha = 0, 1, 2$ but only one of them is a vectorial weight, one has to compute

   $$\int \mathrm{d}^3q\, \frac{\boldsymbol{q}}{q}\,\delta(R-|\boldsymbol{q}|)\,\delta(R-|\boldsymbol{q}+\boldsymbol{r}|)$$

   Switching to spherical coordinates that align the z-axis with $\boldsymbol{r}$ and thus identify the angle between $\boldsymbol{q}$ and $\boldsymbol{r}$ with the latitude ϑ

   $$\int_0^\infty \mathrm{d}q\, q^2\delta(R-q)\int_{-1}^{1}\mathrm{d}(-\cos\vartheta)\int_0^{2\pi}\begin{pmatrix}\cos\varphi\,\sin\vartheta\\ \sin\varphi\,\sin\vartheta\\ -(-\cos\vartheta)\end{pmatrix}\delta(R-\sqrt{q^2+r^2-2rq(-\cos\vartheta)})$$

   which immediately simplifies to

   $$2\pi R^2\int_{-1}^{1}\begin{pmatrix}0\\0\\-u\end{pmatrix}\frac{\delta(u-r/L)}{r} = 2\pi R^2\left(-\frac{r}{L}\right)\frac{1}{r}\frac{\boldsymbol{r}}{r} = -2\pi\frac{1}{4}\frac{r}{L}\left(\frac{2R}{r}\right)^2\boldsymbol{r}$$
   $$= -\frac{\pi L}{2}\frac{\boldsymbol{r}}{r}$$

2. If one of the cross-correlation partners is vectorial and the other is ω_3, then

   $$\int \mathrm{d}^3q\, \frac{\boldsymbol{q}}{q}\,\delta(R-|\boldsymbol{q}|)\,\Theta(R-|\boldsymbol{q}+\boldsymbol{r}|)$$

Omitting the explanation, because it would be redundant with ones already given above, this is how it can be rewritten:

$$2\pi R^2 \int_{-1}^{1} \mathrm{d}u \begin{pmatrix} 0 \\ 0 \\ -u \end{pmatrix} \Theta(u{-}r/L) = -2\pi R^2 \frac{\boldsymbol{r}}{r} \int_{r/L}^{1} \mathrm{d}u\, u = \pi R^2 \left(\left[\frac{r}{L}\right]^2 - 1 \right) \frac{\boldsymbol{r}}{r}$$

Explicit Expressions for the Weight Function Fourier Transforms The weight functions proportional to $\delta(R-r)$ are quickly written down

$$\begin{aligned} \frac{1}{4\pi R^2}\hat{\omega}_2 = \frac{1}{R}\hat{\omega}_1 = \hat{\omega}_0 = \mathcal{F}\left[\frac{\delta(R-r)}{4\pi R^2}\right] \\ &= \int_0^\infty 4\pi r^2 \,\mathrm{d}r \,\mathrm{sinc}(kr)\, \frac{\delta(R-r)}{4\pi R^2} \\ &= \mathrm{sinc}(kR) \end{aligned}$$

The Fourier Transform of ω_3 is given by

$$\begin{aligned} \hat{\omega}_3 &= \mathcal{F}\left[\Theta(R-r)\right] \\ &= \int_0^\infty 4\pi r^2 \,\mathrm{d}r \,\mathrm{sinc}(kr)\, \Theta(R-r) \\ &= 4\pi R^3 \frac{\sin(kR) - kR\, \cos(kR)}{(kR)^3} \end{aligned}$$

The vectorial densities are a bit less straightforward to transform. The idea used here is to choose coordinates for the integrand, in which $\boldsymbol{k}$ is aligned with the z-axis, such that $\boldsymbol{k}/k$ corresponds to $\begin{pmatrix} 0 & 0 & 1 \end{pmatrix}$. Defining $M_1 = R$

and $M_2 = 4\pi R^2$, the computation is as follows:

$$\begin{aligned}
\hat{\boldsymbol{\omega}}_\alpha &= \int \mathrm{d}^3 r \, e^{-i\boldsymbol{k}\boldsymbol{r}} \frac{\boldsymbol{r}}{r} \omega_\alpha(\boldsymbol{r}) \\
&= \int_0^\infty \mathrm{d}r \int_0^\pi r \, \mathrm{d}\vartheta \int_0^{2\pi} r \sin\vartheta \, \mathrm{d}\varphi \cdot e^{-ikr\cdot\cos\vartheta} \begin{pmatrix} \cos\varphi \, \sin\vartheta \\ \sin\varphi \, \sin\vartheta \\ \cos\vartheta \end{pmatrix} \omega_\alpha(r) \\
&= \int_0^\infty 2\pi r^2 \mathrm{d}r \, \omega_\alpha(r) \int_{-1}^1 \mathrm{d}(-\cos\vartheta) \, e^{ikr\cdot(-\cos\vartheta)} \begin{pmatrix} 0 \\ 0 \\ \cos\vartheta \end{pmatrix} \\
&= \frac{\boldsymbol{k}}{k} \int_0^\infty 2\pi r^2 \mathrm{d}r \, \omega_\alpha(r) \int_{-1}^1 \mathrm{d}\kappa \, (-\kappa) \, e^{ikr\cdot\kappa} \\
&= \frac{\boldsymbol{k}}{k} \int_0^\infty 2\pi r^2 \mathrm{d}r \, \omega_\alpha(r) \left(-\frac{1}{ik} \frac{\partial}{\partial r} \right) \int_{-1}^1 \mathrm{d}\kappa \; e^{ikr\cdot\kappa} \\
&= \frac{\boldsymbol{k}}{k} \int_0^\infty 4\pi r^2 \mathrm{d}r \, \omega_\alpha(r) \left(-\frac{1}{i} \frac{\partial}{\partial(kr)} \right) [\mathrm{sinc}(kr)] \\
&= \frac{i\boldsymbol{k}}{k} \int_0^\infty 4\pi r^2 \mathrm{d}r \, \omega_\alpha(r) \frac{kr\cdot\cos(kr) - \sin(kr)}{(kr)^2} \\
&= M_\alpha \cdot \frac{i\boldsymbol{k}}{k} \frac{kR\cdot\cos(kR) - \sin(kR)}{(kR)^2}
\end{aligned}$$

References

[1] J. A. Barker and D. Henderson. “Perturbation Theory and Equation of State for Fluids. II. A Successful Theory of Liquids”. In: *The Journal of Chemical Physics* 47.11 (1967), pp. 4714–4721. DOI: `10.1063/1.1701689`. eprint: `https://doi.org/10.1063/1.1701689`. URL: `https://doi.org/10.1063/1.1701689`.

[2] T. Bernet et al. “Generalization of the Fundamental-Measure Theory Beyond Hard Potentials: The Square-Well Fluid Case”. In: *The Journal of Physical Chemistry C* 121.11 (2017), pp. 6184–6190. DOI: `10.1021/acs.jpcc.7b00797`. eprint: `https://doi.org/10.1021/acs.jpcc.7b00797`. URL: `https://doi.org/10.1021/acs.jpcc.7b00797`.

[3] Norman F. Carnahan and Kenneth E. Starling. “Equation of State for Nonattracting Rigid Spheres”. In: *The Journal of Chemical Physics* 51.2 (1969), pp. 635–636. DOI: `10.1063/1.1672048`. eprint: `https://doi.org/10.1063/1.1672048`. URL: `https://doi.org/10.1063/1.1672048`.

[4] Hendrik Hansen-Goos and Roland Roth. “Density functional theory for hard-sphere mixtures: the White Bear version mark II”. In: *Journal of Physics: Condensed Matter* 18.37 (2006), p. 8413. DOI: `10.1088/0953-8984/18/37/002`. URL: `https://dx.doi.org/10.1088/0953-8984/18/37/002`.

[5] Trell L. Hill. “Statistical Mechanics: Principles and Selected Applications”. In: Dover Publications, Inc., 1956. Chap. 6.

[6] N. David Mermin. “Thermal Properties of the Inhomogeneous Electron Gas”. In: *Phys. Rev.* 137 (5A 1965), A1441–A1443. DOI: `10.1103/PhysRev.137.A1441`. URL: `https://link.aps.org/doi/10.1103/PhysRev.137.A1441`.

[7] B. R. A. Nijboer and L. Van Hove. “Radial Distribution Function of a Gas of Hard Spheres and the Superposition Approximation”. In: *Phys. Rev.* 85 (5 1952), pp. 777–783. DOI: `10.1103/PhysRev.85.777`. URL: `https://link.aps.org/doi/10.1103/PhysRev.85.777`.

[8] Linda E. Reichl. “A Modern Course in Statistical Physics”. In: John Wiley and Sons, Inc., 1998. Chap. 9.

[9] Howard Reiss et al. “Aspects of the Statistical Thermodynamics of Real Fluids”. In: *The Journal of Chemical Physics* 32.1 (1960), pp. 119–124. DOI: `10.1063/1.1700883`. eprint: `https://doi.org/10.1063/1.1700883`. URL: `https://doi.org/10.1063/1.1700883`.

[10] Yaakov Rosenfeld. “Free-energy model for the inhomogeneous hard-sphere fluid mixture and density-functional theory of freezing”. In: *Phys. Rev. Lett.* 63 (9 1989), pp. 980–983. DOI: `10.1103/PhysRevLett.63.980`. URL: `https://link.aps.org/doi/10.1103/PhysRevLett.63.980`.

[11] R Roth et al. “Fundamental measure theory for hard-sphere mixtures revisited: the White Bear version”. In: *Journal of Physics: Condensed Matter* 14.46 (2002), p. 12063. DOI: `10.1088/0953-8984/14/46/313`. URL: `https://dx.doi.org/10.1088/0953-8984/14/46/313`.

[12] Roland Roth. “Fundamental measure theory for hard-sphere mixtures: a review”. In: *Journal of Physics: Condensed Matter* 22.6 (2010), p. 063102. DOI: `10.1088/0953-8984/22/6/063102`. URL: `https://dx.doi.org/10.1088/0953-8984/22/6/063102`.

Erklärung

Hiermit versichere ich, dass ich die vorliegende Arbeit selbstständig verfasst und keine anderen als die angegebenen Quellen und Hilfsmittel benutzt habe, dass alle Stellen der Arbeit, die wörtlich oder sinngemäß aus anderen Quellen übernommen wurden, als solche kenntlich gemacht sind und dass die Arbeit in gleicher oder ähnlicher Form noch keiner Prüfungsbehörde vorgelegt wurde.

Erlangen, den 11.04.2023